Contributions to Zoology, 85 (2) 201-234 (2016)

Triadobatrachus massinoti, the earliest known lissamphibian (Vertebrata: Tetrapoda) re-examined by μCT scan, and the evolution of trunk length in batrachians

Eduardo Ascarrunz[1, 2], Jean-Claude Rage[2], Pierre Legreneur[3], Michel Laurin[2]
[1] *Department of Geosciences, University of Fribourg, Chemin du Musée 6, 1700 Fribourg, Switzerland*
[2] *Sorbonne Universités CR2P, CNRS-MNHN-UPMC, Département Histoire de la Terre, Muséum National d'Histoire Naturelle, CP 38, 57 rue Cuvier, 75005 Paris, France*
[3] *Inter-University Laboratory of Human Movement Biology, University of Lyon, 27-29 Bd du 11 Novembre 1918, 69622 Villeurbanne Cédex, France*
[4] *E-mail: eduardo.ascarrunz@unifr.ch*

Key words: Anura, caudopelvic apparatus, CT scan, Salientia, Triassic, trunk evolution

Abstract

Triadobatrachus massinoti is a batrachian known from a single fossil from the Early Triassic of Madagascar that presents a combination of apomorphic salientian and plesiomorphic batrachian characters. Herein we offer a revised description of the specimen based on X-ray micro-tomography data. We report previously unknown caudal vertebrae, possible mentomeckelians, and hidden parts of other structures. We also confirm the presence of a ventrolateral ledge on the opisthotic, and we rectify some previous interpretations. There are no cervical ribs and the jaw may have had an angular. The presacral region is composed of 15 vertebrae with a unique atlas-axis complex instead of 14 vertebrae with a bipartite atlas. The configuration of the pelvic girdle is not very clear, although it is likely more plesiomorphic than the anuran-like condition previously assumed. Our re-assessment of the saltatorial performance of *Triadobatrachus* supports the traditional interpretation that this animal was not a specialised jumper. In order to assess the sequence of events in the early evolution of the salientian morphotype, we estimated the ancestral length of the trunk region of batrachians under different hypotheses of lissamphibian relationships and divergence times. Most of our results suggest that some trunk reduction took place before the divergence of caudates and salientians (presumably in the Permian), and that the trunk of *Triadobatrachus* mostly reflects this ancestral condition. Thus, trunk reduction possibly preceded the anteroposterior elongation of the ilia and the shortening of the tail seen in *Triadobatrachus*. We also provide an updated review of the data relevant for the use of *Triadobatrachus* as a calibration constraint in molecular divergence age analyses that meets recently-suggested standards.

Contents

Introduction

The earliest undisputed lissamphibians known to date are the Early Triassic (~251 - 247 Ma) salientians (total-group anurans) *Triadobatrachus massinoti* (Piveteau, 1936), of which a single fairly complete specimen has been found, and *Czatkobatrachus polonicus*, Evans and Borsuk-Białynicka, 1998, which is known only by disarticulated remains of the appendages and vertebrae. These two taxa are the only fossil record from Carroll's gap (an expression coined by Marjanović and Laurin [2013], and spanning the Middle Permian to the Early Jurassic) documenting the origin and earliest phases of evolution of lissamphibians.

Under the phylogenetic hypotheses on the origin of lissamphibians currently defended in the literature, lissamphibians are closest relatives to either amphibamid temnospondyls (Ruta and Coates, 2007; Maddin

and Anderson, 2012) or lysorophian lepospondyls (Vallin and Laurin, 2004; Marjanović and Laurin, 2013). In both cases, the most recent possible sister taxa date back to the Cisuralian (Early Permian, 299 - 271 Ma), leaving a temporal gap of at least ~20 My between them and *Triadobatrachus*.

The second and longest part of the gap (at least 47 My) ends with the next earliest salientian (*Prosalirus bitis*, Shubin and Jenkins, 1995) in the Pliensbachian (Early Jurassic, 190.8 - 182.7 Ma), which is morphologically very close to anurans (Shubin and Jenkins, 1995). The first fossils that unambiguously belong to other lissamphibian clades also appear in the Jurassic (Marjanović and Laurin, 2007, 2014). Heckert *et al*. (2012) reported an atlas and putative anteriorly-elongated ilia of possible batrachian affinities from the Upper Triassic Cumnock Formation, North Carolina, but the fragmentary condition of the material precludes a reliable identification, as they themselves warn. As far as we are aware, other possible Triassic lissamphibian material lacks unequivocal diagnostic characters (*e.g*. Ivakhnenko, 1978). Thus, *Triadobatrachus* finds itself in the doubly important position of being the only reasonably complete fossil connecting one of the two major clades of living tetrapods with its possible sister-groups in a span of at least 67 My, and of documenting the early evolution of the highly specialised morphology of anurans.

Preserved as a mould in a small nodule split into two parts, *Triadobatrachus* has been the subject of several descriptive works (Piveteau, 1937; Watson, 1941; Hecht, 1962; Griffiths, 1963; Estes and Reig, 1973; Rage and Roček, 1989; Borsuk-Białynicka and Evans, 2002; Sigurdsen *et al*., 2012), the most recent major description being that of Rage and Roček (1989) (hereafter referred to as RR89). However, because of the type of preservation, those studies have been limited to the difficult examination of the negative impressions left by the skeleton, or to the use of casts. Here we present the first description of the fossil based on X-ray computed microtomography data. This new approach allowed us to reassess its morphology with a three-dimensional model of the reassembled skeleton, and to discover previously unknown structures that were hidden deeper inside the nodule matrix.

Our description reports new characters and updates the information on several features, such as the ventrolateral ledge of the opisthotic, dorsal protuberances of the exoccipital, the morphology of the atlas-axis complex (as two distinct vertebrae rather than a fused complex, no ribs) and its mode of articulation with the skull, the minimal number of caudal vertebrae, and the nature of the sacral articulation, and has implications on the interpretation of the evolution of the peculiar caudopelvic system and the adaptations for jumping of anurans. We also seized the opportunity to assess a more general question regarding the evolution of batrachians (caudates + salientians) in the light of our new discoveries. Our re-examination yields 15 presacral vertebrae for *Triadobatrachus* (instead of the 14 previously reported in RR89), which is well within the range of variation of presacral numbers of caudates (12 or 13 to over 60, figure 10). Therefore, it is possible that the extent of vertebral number reduction and trunk shortening (relative to the ancestral condition of lissamphibians) seen in *Triadobatrachus* is a batrachian synapomorphy rather than a peculiarity of Salientia. This hypothesis is explored below. Finally, we also provide an updated review of the evidence relevant to the use of *Triadobatrachus* as a dating constraint.

Material and methods

The holotype of *Triadobatrachus massinoti* is housed in the palaeontological collection of the Muséum National d'Histoire Naturelle in Paris (MNHN), under the voucher number MNHN.F.MAE126. It consists of a split nodule that exposes the dorsal and ventral halves of the natural mould of the fossil.

Tomography and segmentation

We based our description on X-ray microtomography (XMT) of MNHN.F.MAE126. The two halves of the nodule were placed together in their original position for image acquisition.

XMT was done in a Phoenix X-ray microtomograph (v|tome|x 240 L, GE Sensing & Inspection Technologies) of the AST-RX imaging facilities of the MNHN. Image acquisition was performed under a tension acceleration of 145 kV and current intensity of 420 µA. The X-ray source consists of a microfocus Phoenix 240 kV/320 W open tube. We used a detector composed of a Perkin Elmer flat panel of 40×40 cm, 2024×2024 pixels, and pixel size of 200 µm. The dataset consists of 18000 projections taken over 360° with exposure time of 1 s. The geometry was set to obtain a voxel size of 62.2 µm. The final volume set is 1076×869×2005 pixels.

The resulting tomograms were rotated to be oriented in the standard anatomical planes and the space

surrounding the fossil was cropped using the program FIJI (Image J 2.0). The rotation modified the voxel size by about 10%.

Image segmentation was performed on MIMICS® v. 16 (Materialise) at the 3D imaging platform of the MNHN. We first applied automatic thresholding to isolate the cavity within the nodule. That initial segmentation was later refined by several passes of slice-by-slice manual inspection and correction along the three standard anatomical axes. Although the nodule cavity has a good contrast against the nodule matrix, the segmentation process is not without challenges. Notably, it is often difficult to isolate the skeleton imprint from the surrounding soft tissue imprint and the fracture of the nodule. The 3D model we present in this article is our interpretation.

The 3D models produced on MIMICS were exported in binary stereolithography format. Based on those 3D models, we also reconstructed the articulated pelvic girdle of *Triadobatrachus* on Blender v. 2.72b (2014). All visualisations were rendered in MeshLab v. 1.3.3 (Cignoni and Ranzuglia, 2014).

The raw tomography data remain property of the MNHN, and they are available upon request through the 'colhelper' system (http://colhelper.mnhn.fr/). The 3D models produced and described in this study are available as the online supplementary information.

Other material examined

Besides the original fossil and the X-ray images, we studied rubber casts, as RR89 did. Several fine details on the surface of the bones can sometimes be better appreciated on the casts. We also took UV photographs of the fossil (Online supplementary information 1), but they did not reveal any novel details and will not be discussed here further.

Evolution of trunk length

We studied trunk length evolution using two traits: the number of presacral vertebrae and the ratio between the length of the presacral region of the vertebral column and the maximum width of the skull (PSL/SW ratio). Atlas and 'axis' are strictly speaking parts of the cervical region rather than the trunk, but since these two regions are not distinct in anurans, we consider all presacral vertebrae as part of the 'trunk' region in this study. The data on the number of presacral vertebrae come mostly from the literature and the observation of a few specimens (online supplementary information 2). The number of presacral vertebrae is variable within some lissamphibian species, especially caudates and gymnophionomorphs (Litvinchuk and Borkin, 2003; Lanza *et al*., 2010). For example, *Triturus cristatus* (Laurenti, 1768) has between 13 and 16 presacrals, and elongated forms such as *Proteus anguinus* Laurenti, 1768 tend to have greater ranges (27-35; Lanza *et al*., 2010). Therefore, here we chose to use the mode value, when available. For fossils where there is uncertainty in the number of presacrals, we used the average between the plausible values when the identity of the sacral vertebra is uncertain. Recent caecilians lack sacra and pelves altogether, so we used the pre-cloacal vertebrae instead. We selected 83 lissamphibian, nine lepospondyl, and ten temnospondyl taxa. Special care was taken to include extinct forms stratigraphically and phylogenetically close to the origin of Batrachia.

Because the elongation of centra can affect the length of the trunk, it is important to take into account body proportions as well. In order to do this, we quantified relative trunk length as PSL/SW ratio. The decision to use the width of the skull was taken because it can be approximately measured in *Triadobatrachus*, whereas the full length of its skull cannot be measured. Unfortunately, this precludes the direct comparison with other studies that use the more traditional trunk length/skull length ratio, but its interpretation is still relatively straightforward: low PSL/SW ratios correspond to stocky body forms, of which frogs represent the extreme because of their wide skulls in addition to their short trunks. High ratios correspond to slender body forms with long trunks; gymnophionans and many lepospondyls occupy this end of the spectrum. A few taxa with unusual body forms (*e.g. Diplocaulus*) can complicate this generalisation, but we believe it to be mostly valid for our sample.

Presacral region length and maximum skull width are rarely reported, so we took measurements from images of lissamphibian (n = 56), temnospondyl (n = 7), and lepospondyl (n = 6) skeletons, using Adobe Photoshop CS6 and ImageJ v.1.4. The main sources of our data are the DigiMorph digital library, photographs of specimens of the collection of comparative anatomy of the MNHN, and photographs and diagrams found in the primary literature, especially in the case of fossils. Because of the eclectic nature of our sources and their variable fidelity, these measurements represent rough estimates. A detailed account of the sources can be found in Online supplementary information 6.

Ancestral character estimation of trunk length

We estimated ancestral values for the number of presacral vertebrae of several lissamphibian and possible stem-lissamphibian clades using the fastAnc function of the R package phytools version 0.4-31 (Revell, 2012). This function implements an algorithm of iterative rerooting and calculation of phylogenetically independent contrasts to compute ancestral value estimates that approximate the maximum likelihood solution. Direct maximum likelihood estimation could not be done because the branch length transformations that we performed (see below) yielded numerically singular variance-covariance matrices. Both the number of presacral vertebrae and the PSL/SW ratio were modelled as continuous variables.

We performed our analyses on two topologies, one representing the lepospondyl hypothesis (LH; Marjanović and Laurin, 2013), and another the temnospondyl hypothesis (TH; Ruta and Coates, 2007). The internal topology and branch lengths of Lissamphibia are based on the supertree of Marjanović and Laurin (2014), with minor updates and substituting terminals for stratigraphically and phylogenetically equivalent taxa as required to match our presacral vertebrae number dataset, where required. Temnospondyl topology follows Schoch (2013). The phylogenetic position of the amphibamid temnospondyl *Gerobatrachus hottoni* Anderson *et al*., 2008 is controversial (Marjanović and Laurin, 2008; Sigurdsen and Green, 2011; Marjanović and Laurin, 2014); in the phylogeny that represents the TH, we have placed it as sister to Lissamphibia as suggested by the latest major phylogenetic analysis supporting TH (Maddin and Anderson, 2008). We also placed the albanerpetontid *Celtedens ibericus* McGowan and Evans, 1995 in the basal polytomy of Lissamphibia, as the phylogenetic position of albanerpetontids as either stem-lissamphibians, stem-batrachians, or sister to caudates or gymnophionomorphs is still unclear (Ruta and Coates, 2007; Marjanović and Laurin, 2008; Maddin and Anderson, 2012).

In order to take into account the uncertainty about the divergence age estimates of the nodes of interest, we performed the analyses on five sets of divergence age estimates for Lissamphibia and Batrachia (Table 1), taken from molecular analyses (Marjanović and Laurin, 2007; Zhang and Wake, 2009; San Mauro, 2010; Pyron, 2011), from a stratigraphic fit on the palaeontological data only (using the method described below), and from a compromise between them all, which is close to the molecular estimates obtained by Marjanović and Laurin (2007) using optimal smoothing factors (Marjanović and Laurin, 2007, table 2, row 3).

Other than as indicated above, the branch lengths of the trees correspond to time units as estimated from the fossil record; we used the bin_timePaleoPhy of the geoscale R package version 2.5 (Bapst, 2012), following the criteria for building the supertree of Marjanović and Laurin (2007): internal branches have a minimum length of 3 My and terminal branches span at least the whole oldest stratigraphic unit in which the taxon was found (setting the bin_timePaleoPhy option add.term as TRUE). We did not assess the effect of stratigraphic uncertainty as proposed by Bapst (2013), because preliminary tests showed the computation times for the whole analytical workflow to be prohibitive. Bapst (2014) showed that his 'cal3' time-scaling method provides less biased estimates of rates of trait evolution than the minimum branch length approaches similar to the one used here. However, we do not have the detailed stratigraphic information to calculate the three rates that his method requires. When an analysis required strictly dichotomous trees, we arbitrarily dichotomised polytomies with zero-length branches.

Table 1. Sets of divergence age estimates. We selected six sets of divergence age estimates for the nodes Lissamphibia and Batrachia to assess the sensitivity of ancestral character estimations to different branch lengths. Set 1 is a compromise between the ages of sets 2 to 6, and it is also close to the molecular dates obtained with optimal smoothing factors by Marjanović and Laurin (2007: table 2, row 3). Set 2 corresponds to the values obtained from a stratigraphic fit with minimal internal branch lengths set to 3 My (see Materials and methods for details). Set 3 was taken from molecular estimates of Marjanović and Laurin (2007: table 2, row 4.2), but the divergence date of Batrachia was set to 247.2 Ma instead of their result of 246 Ma, because the original date is incompatible with the age of *Triadobatrachus* used in this study. The cause of this discrepancy is that the upper limit of the Olenekian is older in the latest version of the chronostratigraphic scale. Sets 4, 5, and 6 were taken from Pyron (2011), Zhang and Wake (2009), and San Mauro (2010) respectively. All dates in Ma.

Set	*Lissamphibia*	*Batrachia*	Reference
1	280	260	Compromise
2	260.2	257.2	Stratigraphic fit
3	267	247.2	Marjanović and Laurin (2007) 4.2 modified
4	306	292	Pyron (2011) 1-clock model
5	294	264	Zhang and Wake (2009)
6	315	290	San Mauro 2010

The maximum likelihood approximation of the fastAnc function of phytools assumes a Brownian motion (BM) model of evolution for the continuous character under the same rate of evolution along the entire tree. However, it is evident that this character follows different regimes of evolution between clades of amphibians. While there is great variability in trunk length among caudates, salientians are extremely conservative in having a very short trunk, and gymnophionomorphs have always long body forms. Models of evolution more complex than single-rate BM could better describe this variation. A plausible model, for instance, would be having the base of the tree evolving under BM and local Ornstein-Uhlenbeck regimes in the clades Gymnophionomorpha and Salientia, but we could not fit such a complex model, as explained below.

We conducted preliminary tests trying to fit our trees to Ornstein-Uhlenbeck models with multiple local attractors using the OUwie R package version 1.43 (Beaulieu *et al*., 2012), but we were unable to obtain reliable results from this method (widely different parameter estimates between runs, and the values of the θ parameter were often outside the empirically observed range of variation), in part likely because of insufficient sample size. Therefore, we opted for fitting simpler multirate BM models using the brownieREML function of phytools, an R implementation of the 'non-censored method' of the program Brownie (O'Meara *et al*., 2006). We fitted six models with different combinations of local rates of trunk length evolution in different regions of the tree, as indicated in Table 2. These regions are broad, and were delimited according to the characteristic trunk length of the taxa they encompass.

Table 2. Akaike weights of rate shift models fitted to two topologies and alternative sets of divergence ages. Each rate shift model corresponds to single or multiple regions of the phylogeny that present a local rate of evolution of a trait distinct from the overall rate of the tree, or a single rate for the entire tree (1 rate). We fitted six rate shift models to the presacral vertebrae number data under LH (A) to allow different combinations of local rates for 'short-body' forms (Salientia except *Triadobatrachus*), for gymnophionomorphs, and for lepospondyls. Four models were fitted to the number of presacral vertebrae data under the TH (B), using the same groups as before except lepospondyls, which are not included in this tree. Because we lack measurement data for gymnophionomorphs, fewer models were fitted to the presacral length/skull width ratio data (C and D). The Akaike weights were computed using the small sample correction of the Akaike information criterion. Values indicating best fits (greater weights) are indicated in bold. Note that in all cases, the best model got an Akaike weight over 0.7. The divergence age estimates set numbers correspond to those of table 1. short, Salientia excluding *Triadobatrachus*; lepo, lepospondyls; gym, Gymnophionomorpha; k, number of parameters of the model.

A. NPSV LH	k	Set 1	Set 2	Set 3	Set 4	Set 5	Set 6
lepo	3	0	0	0	0	0	0
gym	3	0	0	0	0	0	0
short	3	0	0	0	0	0	0
lepo + gym	4	0	0	0	0	0	0
lepo + gym + short	**5**	**1**	**1**	**1**	**1**	**1**	**1**
1 rate	2	0	0	0	0	0	0
B. NPSV TH							
gym	3	0	0	0	0	0	0
short	3	8.18×10^{-9}	2.12×10^{-9}	3.96×10^{-9}	1×10^{-9}	3.05×10^{-9}	8.42×10^{-9}
gym + short	**4**	**1**	**1**	**1**	**1**	**1**	**1**
1 rate	2	0	0	0	0	0	0
C. PL/SW LH							
lepo	3	0	0	0	0	0	0
short	**3**	**0.80**	**0.74**	**0.74**	**0.83**	**0.77**	**0.72**
lepo + short	4	0.24	0.26	0.26	0.17	0.23	0.28
1 rate	2	0	0	0	0	0	0
D. PL/SW TH							
short	**3**	**1**	**1**	**1**	**1**	**1**	**1**
1 rate	2	0	0	0	0	0	0

We did not evaluate different possible positions for the rate shift along each branch; instead, we arbitrarily placed the rate shift at the middle of the branch. Model fit was evaluated using the small-sample weights of the corrected Akaike information criterion (AIC), as the number of samples (terminals in the tree, in this case) was less than forty times the number of parameters in all models. When a multi-rate model was selected, we scaled the branches of the tree regions with a local rate by a factor equal to the ratio between the rate of that tree region and the rate of the rest of the tree (Reece and Mehta, 2013) to infer ancestral values. This transformation procedure produced the numerically singular matrices mentioned above.

It should be noted that ancestral state reconstructions of ancient nodes without a dense fossil record tend to yield extensively overlapping of 95% confidence intervals of neighbouring nodes. We believe that the mean nodal estimates can provide a useful rough picture of the pattern of evolution of traits, but we made no attempt to do a formal statistical test of our hypotheses, because such a test is likely to be severely underpowered.

Systematic palaeontology

Amphibia Linnaeus 1758
Lissamphibia Haeckel 1866
Batrachia Latreille 1800
Salientia Laurenti 1768
Triadobatrachus massinoti (Piveteau 1936)

1936a *Protobatrachus* nov.sp., Piveteau, p.1607.
1936b *Protobatrachus Massinoti*, Piveteau, p. 1804.
1938 *Protobatrachus triassicus* n. sp., Kuhn, p. 8.
1962 *Triadobatrachus* nov., Kuhn, p. 328 – (*Protobatrachus* Piveteau, 1937, non Gistl, 1848; non *Probatrachus*, Peters 1878).

Holotype. MNHN F.MAE.126.
Type locality. Near Betsiaka village, Ambilobe Basin. Diana Region, Northwestern Madagascar.
Type horizon. Shale beds equivalent to the Middle Sakamena Group (Lehmann *et al*., 1959). Late Induan - early Olenekian, Early Triassic.

Triadobatrachus is often placed in the taxon Triadobatrachidae (Kuhn, 1962). We are aware of only one instance in the technical literature in which another species –*Czatkobatrachus polonicus*– has been attributed to this family: Carroll's (2007) article on the ancestry of lissamphibians. Carroll (2007: 119) cites Roček and Rage (2000a) as the authorities for that attribution, but that taxonomic opinion is found neither in Roček and Rage (2000a), nor elsewhere in their writings. Therefore, we consider Carroll's familial attribution to be in error. Moreover, we are not aware of any phylogenetic analysis that has retrieved *Triadobatrachus* and *Czatkobatrachus* as sisters in exclusion of the rest of the Salientia (cf. Gao and Wang, 2001; Gao and Chen, 2004; Wang 2004; Dong, *et al*. 2013). Thus, there is no support for a monophyletic Triadobatrachidae under Carroll's (2007) conception of the taxon. We regard Triadobatrachidae as monotypic and therefore redundant.

Geological context and age

Piveteau (1937) indicated that the fossil was found by Adrien Massinot near the village of Betsieka (modern orthography: Betsiaka or Betsihaka) in the Ambilobe basin, in what is now the Ambilobe district of the Diana Region, Northwest Madagascar.

According to Piveteau (1937), the fossil comes from actinopterygian-bearing beds corresponding to either level 4 or 5 of the Lower Triassic succession of the region described by Besairie (1932). The beds are of littoral origin, but they also contain abundant continental material, including plants, suggesting regressive periods.

On the basis of previous studies on the actinopterygian and stegocephalian faunas of the beds, RR89 concluded that the beds correspond to the Middle Sakamena group, to which they assigned a Gyronitian (Induan) age following Besairie and Collignon (1960).

Cosgriff (1984) studied the temnospondyl faunas of the Middle Sakamena group, and assigned them to his 'A1' faunal horizon, which is equivalent to the *Lystrosaurus* Assemblage Zone of the Karoo, South Africa (base of the Induan - early Olenekian). Lucas (2010) reassessed the work of Cosgriff (1984), but he gave apparently contradicting opinions on the age of the Middle Sakamena group (cf. Lucas, 2010 p. 455 versus p. 477).

Shen *et al*. (2002) provide additional stratigraphic information, but they work with a different division of the sedimentary beds, citing Besairie (1972), not Besairie (1932). In this alternative scheme, the actinopterygian-bearing beds associated to *Triadobatrachus* correspond to levels 3 and 4. Shen *et al*. (2002) reported the finding of the conchostracan *Euestheria (Magniestheria) truempyi* Kozur and Seidel, 1983, in what

they believed was probably level 4 of Besairie's (1972) succession (the specimens were not collected in situ). This species was associated to a faunal turnover at the base of the Olenekian in the uppermost Bernburg Formation of the Germanic basin (Shen *et al*., 2002; Kozur, 2006). The underlying level 3 bears fossils of the bivalve *Claraia* Bittner, 1901, which are 'undoubtedly Gandarian' (=Dienerian, late Induan) (Wignall and Twitchett, 2002; Kozur, 2006), and the overlying level 5 bears the ammonoid *Flemingites* Waagen, 1892 of the early Smithian (earliest Olenekian). Thus, the uncertainty of whether *Triadobatrachus* belongs to level 3 or 4 sets a plausible age range of latest Induan-earliest Olenekian (Dienerian - Smithian).

Description

General appearance of the reassembled nodule

The elliptic nodule is about 12 cm in length, with protuberances surrounding the tips of the limbs of the animal. The general reddish-ochre colouration of the nodule suggests a ferruginous composition (Fig. 1). Internally, the X-ray images (Fig. 2) show that the nodule has fine laminations, and that the density distribution of the matrix has a general concentric pattern characterised by a low-density halo in the periphery of the nodule and a gradient that progresses from high density to low density towards the centre. Dispersed

Fig. 1. Dorsal (left) and ventral (right) parts of the nodule containing the fossil. Major divisions of the scale are in cm.

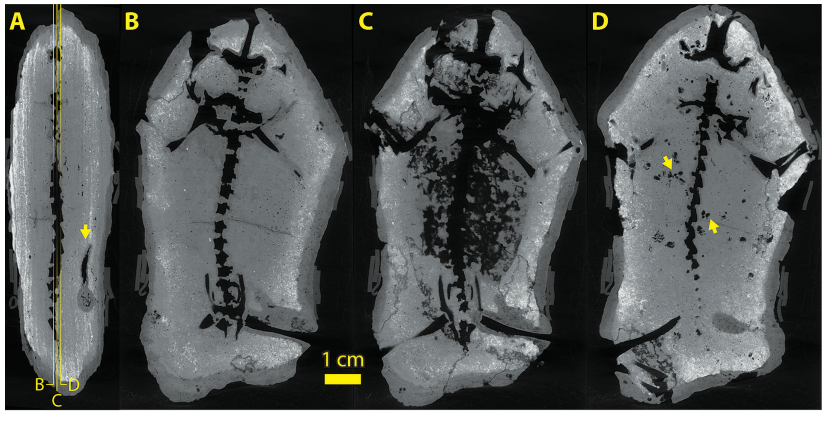

Fig. 2. Selected tomograms (slices) of the scan. A, near-sagittal section (dorsal side to the left); B, parafrontal section ventral to the fracture plane; C, parafrontal section intersecting the fracture plane; D, parafrontal section dorsal to the fracture plane. The yellow lines in A indicate the position of the sections B-D; the arrow indicates a fossil fragment of vegetal material. Note the body halo, particularly around the left hindlimb in B-D, and the soft body impression continuous with the fracture gap and the bone imprint in C. Arrows in D indicate possible remains of gastropod shells.

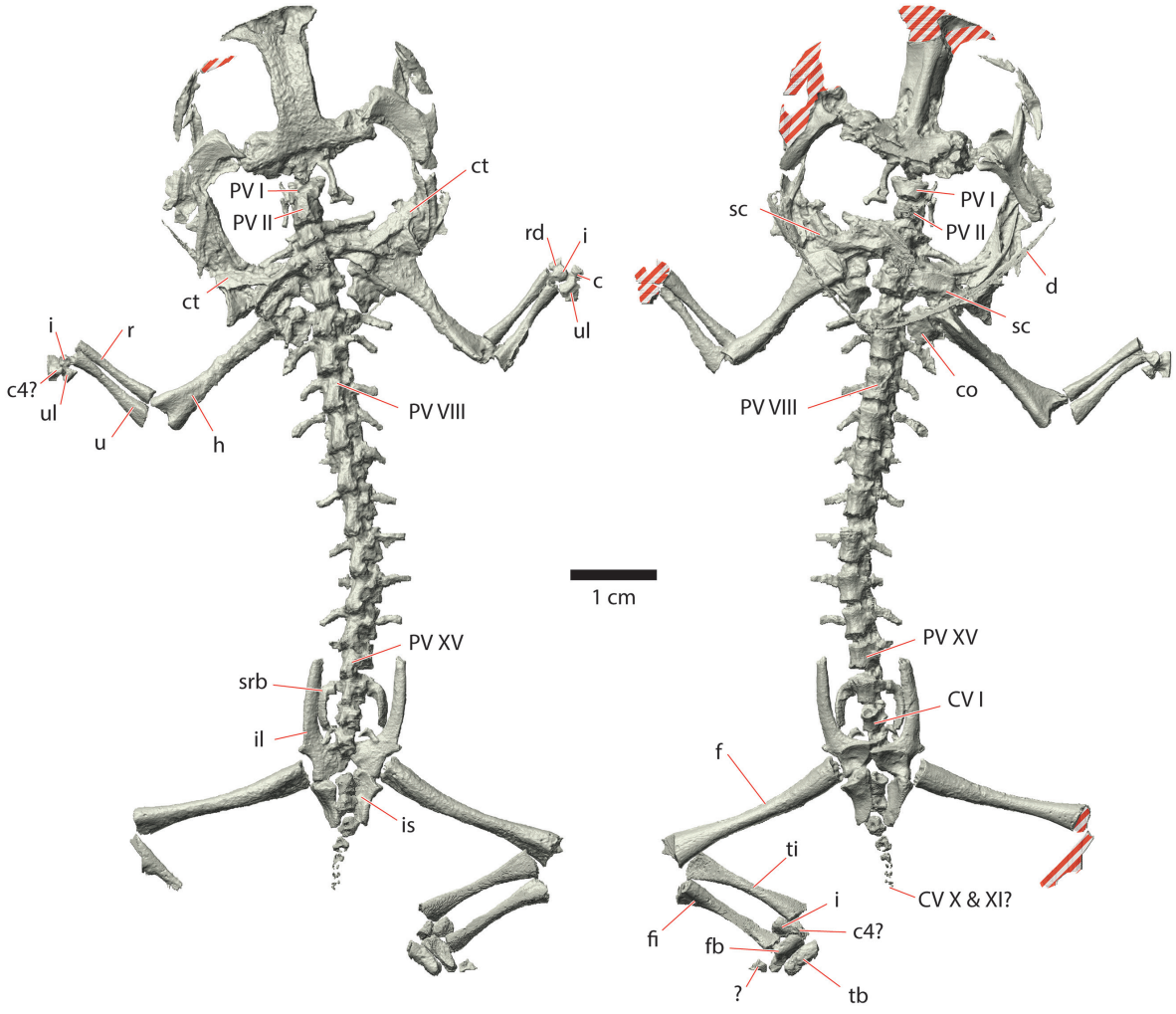

Fig. 3. Dorsal (left) and ventral (right) views of the 3D model. We warn that between presacral vertebrae VIII and XV, the precise shape and length of the ribs is very difficult to determine; our reconstruction of these ribs is generally an approximation. The red-white stripe pattern is used to shade areas where the anatomical structures were not preserved in one of the views. c, centrale; co, coracoid; ct, cleithrum; CV, caudal vertebra; d, dentary; f, femur; fb, fibulare; fi, fibula; h, humerus; i, intermedium; il, ilium; is, ischium; PV, presacral vertebra; r, radius; rd, radiale; sc, scapula; srb, sacral rib; tb, tibiale; ti, tibia; u, ulna; ul, ulnare.

within the matrix, numerous small (a few mm in maximum length and generally flattened) vacuities are found, many of which are probably moulds of gastropod shells. The second largest fossil in the nodule is a fragment of vegetal material in the dorsal part.

The imprint of the soft body is often confluent with the imprint of the skeleton, partially obscuring skeletal anatomy. The contour of the soft elements is clear only in the trunk region. Deeper into the matrix, there are no further traces of soft tissue, except perhaps a low-density halo around the left femur.

Skull

Exocranium

Phylogenetic bracketing indicates that praemaxillae, septomaxillae, and vomers were most likely present in *Triadobatrachus*, but these elements correspond to the snout region, which lies outside the nodule. Thus, they are not preserved in the fossil.

The frontoparietal of *Triadobatrachus* has been extensively discussed in the preceding literature. Piveteau (1937) and Watson (1941) described a longitudinal

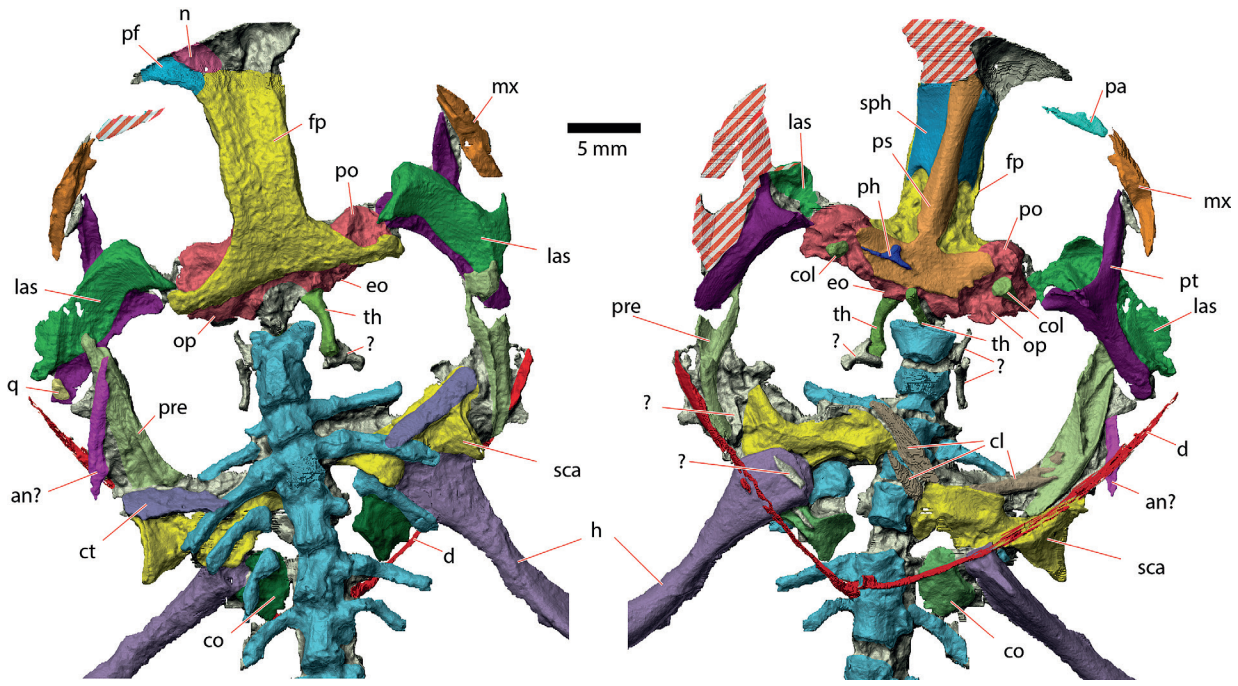

Fig. 4. Dorsal (left) and ventral (right) views of the skull and pectoral girdle. The images have been colourised to reflect our anatomical interpretations. The red-white stripe pattern is used to shade areas where the anatomical structures were not preserved in one of the views. an, angular; cl, clavicle; ct, cleithrum; co, coracoid; col, columella; d, dentary; eo, exoccipital; fp, frontoparietal; h, humerus; las, lamella alaris squamosi; mx, maxilla; n, nasal; op, opisthotic; pa, palatine; pf, prefrontal; ph, parahyoid; po, prootic; pre, prearticular; ps, parasphenoid; pt, pterygoid; q, quadrate; sca, scapula; sph, sphenethmoid; th, thyrohyal. The line indicating the prootic in the dorsal view also indicates the epiotic eminence.

suture line, and thus considered this bone to be paired. For Hecht (1962), the extent of the longitudinal line was limited to the posterior region. RR89 agreed with Hecht's observation and they concluded that this feature reflects an incomplete fusion of the frontoparietals, in accordance with their interpretation of the specimen as a postmetamorphic juvenile rather than an adult. Estes and Reig (1973) made no mention of this feature, but the frontoparietal is illustrated as a single bone in their article (Estes and Reig, 1973: fig. 1-13). On the 3D visualization we can observe both a median inflexion throughout the whole length of the bone, which is more pronounced in its posterior half, and a slight horizontal inflexion at the mid-orbital level. Unfortunately, no suture lines are apparent on the 3D visualization, neither between left and right portions of the frontoparietal nor between the frontoparietal and the anterior bones of the dermatocranium (viz. nasal and ?prefrontal). Under direct examination of the fossil, the longitudinal inflexion is more evident, with a line between left and right frontoparietals. However, we are not certain that this line represents a bone suture; it might also be an artefact of the low and irregular ornamentation that is present on the entire surface of this bone. RR89 reported a pineal foramen, which is visible as a small concavity immediately posterior to an irregular elliptical structure. This foramen is also another potential artefact produced by the ornamentation pattern.

Just anterior to the prootic region, the frontoparietal bears short laminae perpendiculares ('ventral flanges', in RR89). In its posterior region, the frontoparietal has rather long lateral processes that extend over the otic capsules, reaching just over the crista parotica.

As described by RR89, a triangular, irregular structure situated anterior to the frontoparietal is probably of sedimentary origin. To the left of this structure, two triangular elements are the nasal (more medially situated) and possibly the prefrontal (more lateral, forming part of the orbital margin). There seem to be one or more cranial elements where the right nasal should be, but the preservation is too poor to allow any identification.

The parasphenoid bears a long and slender cultriform process, whose tip is not preserved. The lateral margins of the cultriform process are concave in the

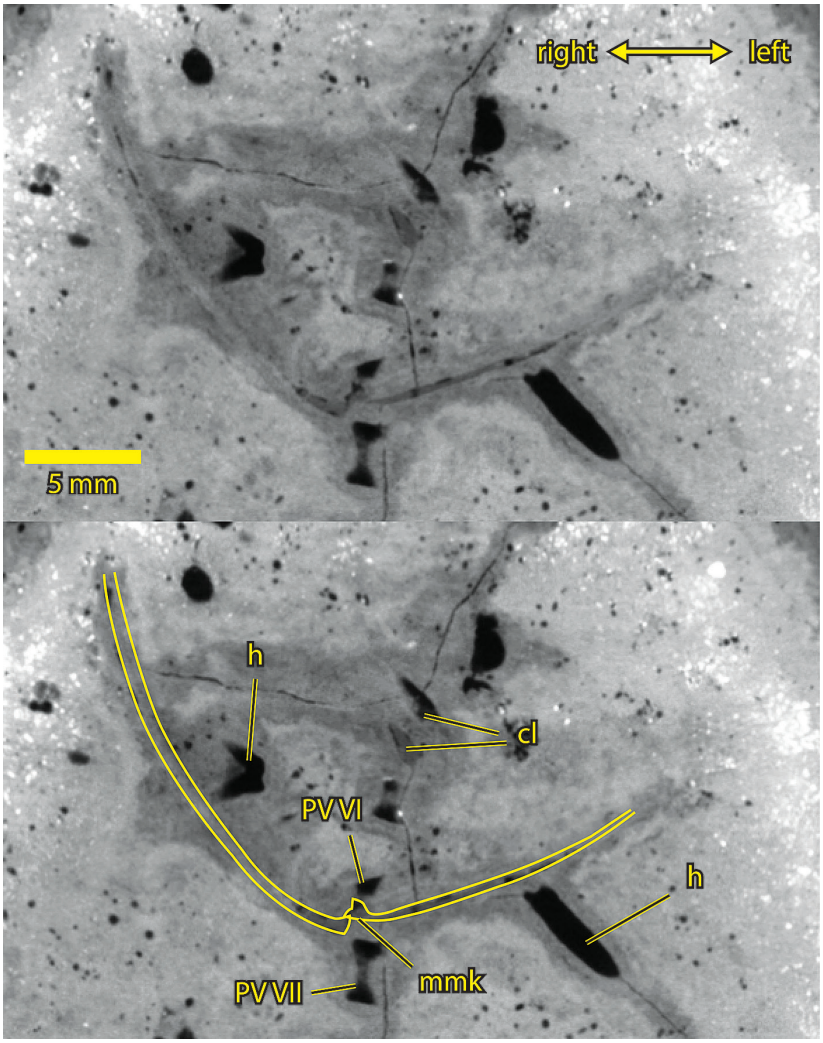

Fig. 5. Section of a tomogram showing the symphyseal region of the dentaries (top) and the same image with a superimposed interpretative drawing (bottom). Note the medially-directed pointed structures on the left mentomeckelian ossification, which is probably fused to the dentary. The contrast of the tomogram has been enhanced for clarity. cl, clavicle; h, humerus; mmk, mentomeckelian; PV, presacral vertebra.

sphenethmoidal region. The posterior part of the parasphenoid bears lateral alary processes, whose tips border the region that likely corresponded to the fenestra ovalis. The posterolateral angle of the left alary process seems to bear a curved notch, but this is could merely be a part that broke off.

On both sides, squamosals and pterygoids are preserved in very close contact; in some regions it is difficult to determine whether certain structures belong to one or the other. The squamosal and pterygoid of the left side were displaced anteriorly from the neurocranial articulation. The wide dorsal lamina of each squamosal (lamella alaris squamosi) has a complex form, and bears articular processes on its dorso-medial tip. A narrow, crescentic region on the antero-dorsal border of the lamella alaris squamosi features a very shallow ornamentation (barely visible on the 3D visualisations, more apparent on the fossil and the casts). Posteriorly, the lamella alaris squamosi forms a broad concave surface that is devoid of ornamentation. RR89 interpreted it as a zone of muscle insertion. The posterolateral process of the squamosals cannot be observed on the 3D visualisations, although its presence is expected because in anurans it encloses the palatoquadrate together with the posterolateral ramus of the pterygoid. It is not visible, perhaps, because in ventral view, the pterygoid lies over the region where it could have been found. On the figure 2A of RR89 there is an unidentified element (labelled '?'), which is covered by the lamella alaris squamosi in such a way that only the posterior margin of the unidentified element can be seen, running parallel to the posterior margin of the

lamella alaris squamosi. This element actually corresponds to the posteromedial margin of the pterygoid, as suggested by Piveteau (1937: fig. 7).

As in anurans, the pterygoids of *Triadobatrachus* feature three rami (Roček, 1981): an anteriorly-directed ramus maxillaris, a postero-lateral ramus posterior (also known as the quadrate ramus), and a medially-directed ramus interior. Additionally, there is a ventromedial process; it is prolonged by ridges that extend well onto the ramus interior and the ramus posterior (Fig. 4; 3D model 1 in the on-line supplement S2). Only the base of the ventromedial process is preserved; the tip got broken off in both pterygoids. RR89 described these structures as 'deep and thin lamellae [that] extend ventrally from the rami interiores of the pterygoids', but Rage (2006) described it more clearly as a 'processus ventral du ptérygoïde, dont l'extension reste inconnue' ('ventral process of the pterygoid of unknown extension'). To our knowledge, this ventromedial process is unique amongst the Stegocephali Cope, 1868 sensu Laurin (1998) (*i.e.*, all choanates more closely related to Temnospondyli than to *Panderichthys*).

A process connects the ventral surface of the left lamella alaris squamosi and the margo orbitalis of the left pterygoid. RR89 suggested that this might correspond to the posterolateral process of the squamosal, which would be fused to the pterygoid. If this is the posterolateral process indeed, then it is also possible that it was crushed against the pterygoid, and thus this contact between the two bones would be artefactual. The tomography does not settle this issue.

Báez and Basso (1996) suggested that the elements that were interpreted as the rami maxillares of the pterygoid by RR89 could be quadratojugals. The 3D visualisations confirm the original interpretation of RR89.

The left palatine is a small, transversally-oriented bone visible in the anterior half of the orbit. RR89 concluded that it has probably been displaced posteriorwards. As in anurans, the palatine is edentulous.

On the casts, only the posterior ends of the maxillae are preserved, just about the border of the nodule. In addition, the tomography revealed a portion of maxilla at the anterior margin of the right orbit; a part of the lamina horizontalis may be discerned. Although the maxillae are more visible on the 3D visualisations than on the casts, there are no indications of the presence of teeth. Still, the preservation of these bones is very poor to consider this definitive evidence of lack of maxillary teeth.

The mandible is disarticulated, rotated ~170° postero-ventrally, and slightly displaced anteriorly; in the following description we refer to the normal anatomical, rather than the post-mortem, distribution of the elements. The posteriormost bones on each side of the mandible were referred to as 'praearticulars sensu lato' in RR89, as they resemble the prearticular bone of caudates in having a clear mandibular fossa. The exact homology of this bone remains unclear, and we retain their use of the name 'prearticular' here only for simplicity. It seems straightforward to consider it homologous to the so-called 'angulosplenial' bone of anurans, which is considered by some to be the angular because it develops from a single ossification centre in most anurans (Z. Roček pers. comm). However, this interpretation is complicated by the possible presence of an independent angular (see below). Further discussions on the homology of this bone should take into account the embryological evidence and the competing phylogenetic hypotheses on the origin of lissamphibians, but will remain limited by the quality of the preservation of the mandible of the fossil.

Both prearticulars show a furrow on their ventral or ventrolateral surfaces (exposed in the dorsal cast, Fig. 4), in which RR89 deduced that Meckel's cartilage was housed and was covered by the dentary. Lying dorsal and oblique to the left prearticular, the long element that was considered part of the prearticular in RR89 could be an angular instead. Such an angular could have been originally housed within the ventral furrow of the prearticular. The right prearticular shows a large opening in medial view, which is not present in the left prearticular (3D model 1). Therefore, it is likely damage and not an exomeckelian fossa.

The dentaries are very long, extending posteriorly far more than in most anurans (Fig. 4). Only the ventral part of the left dentary can be directly observed on the fossil; the tomographic data allow us to make a much more complete reconstruction. Most of the dentaries are preserved as regions of slightly different density from the surrounding matrix, not as cavities in the nodule. There are no indications of the presence of teeth. The mandibular symphysis is slightly disarticulated, with the symphyseal extremities lying just ventral the sixth vertebra. Each symphyseal extremity is expanded, conical and produces a lingual projection (Fig. 5). These projections are probably part of the cupule formed by the mentomeckelian ossification (*i.e.* infrarostrals according to Roček 2003) that holds the pads of connective tissue of the mandibular symphysis in many anurans, as seen in the hylid frog *Acris crepitans*

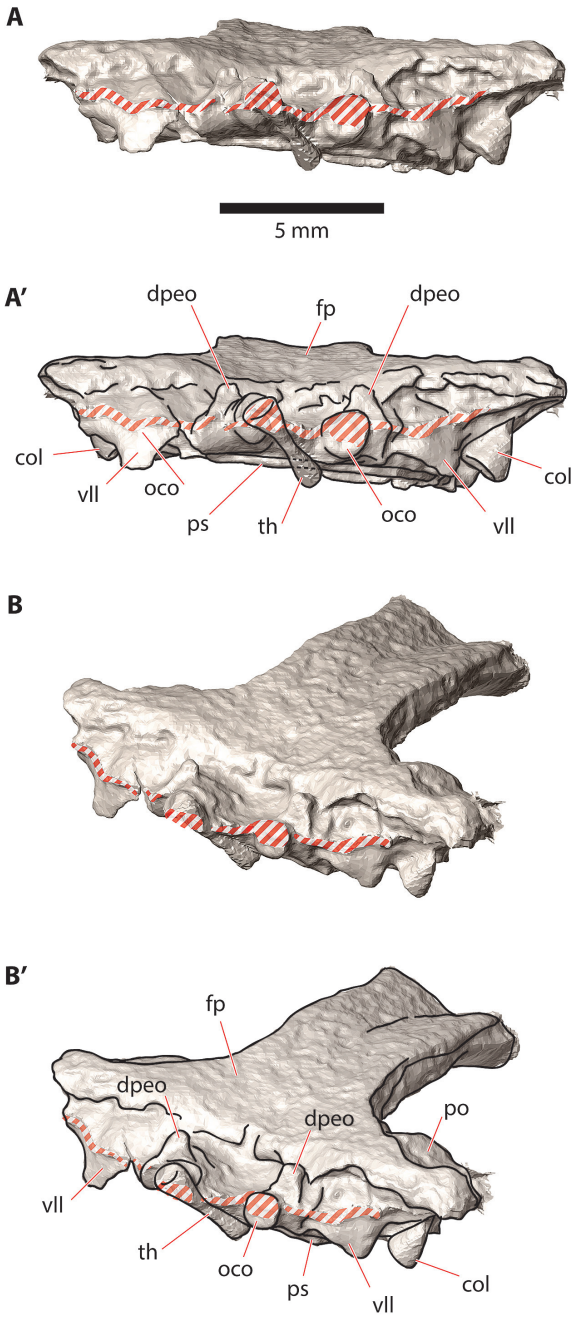

Fig. 6. Visualisations of the occipital region in occipital (A) and oblique (B) views, and corresponding interpretative drawings (A' and B', respectively). The red-white stripe pattern is used to shade areas where the anatomical structures were not preserved in one of the views. The dashed lines indicate the continuation of the parasphenoid behind the thyrohyal. col, columella; dpeo, dorsal protuberance of the exoccipital; fp, frontoparietal; oco, occipital condyle; po, prootic; ps, parasphenoid; th, thyrohyal; vll, ventrolateral ledge of the opisthotic.

Duméril and Bibron, 1841 (Maglia *et al.*, 2007: fig. 10) and the ranoid *Thaumastosaurus gezei* Rage and Roček, 2007 (Laloy *et al.*, 2013: fig. 4E). As these two projections are continuous with the dentaries, we hypothesise that the mentomeckelian ossification was fused to the dentaries. However, another plausible interpretation is that the lingual projection is a salient of the dentary itself. Such lingual salients are sometimes present in temnospondyls (*e.g. Edingerella madagascariensis*, J-C Rage pers. obs.)

Endocranium

The sphenethmoid is preserved only posterior to the planum antorbitale. Its anatomy does not differ from that of anurans. Between the sphenethmoid and the prootics, the lateral braincase walls were not ossified. The prootic foramina do not seem to have been delimited by bone.

The anatomical interpretation of the remains of the otic capsules is challenging, as left and right structures differ in their states of preservation. The following description of the otic region is mostly novel. The 3D visualisations allow us to observe that most of the left part of the endocranium has been dorsoventrally compressed postmortem. This is most evident in occipital view, as shown by the inclination of the parasphenoid with respect to the frontoparietal (Fig. 6A and A'). The elements of the left otic capsule are also more spread than what is seen on the right side (Fig. 4). Thus, the left otic capsule is probably crushed and disarticulated to some degree.

RR89 indicated the presence of separate prootics, exoccipitals ('occipitale laterale' in RR89) and opisthotics. The prootics are large and form the whole anterodorsal wall of the otic capsule; the epiotic eminence is clearly visible dorsally (Fig. 4). The opisthotics are smaller and form part of the posterior wall of the otic capsule. This wall bears the ventrolateral ledge that can be found in anurans and in the Early Permian temnospondyl *Doleserpeton annectens* Bolt, 1969 (Sigurdsen, 2008) (Fig. 6A and A'). Sigurdsen (2008) had tentatively suggested its presence in *Triadobatrachus*, and we confirm it. RR89 indicated that a part of the right opisthotic was broken off. That interpretation is supported by the comparison with the shape of the left opisthotic and the presence of possible fracture marks. On the right otic capsule, a concavity is located latero-ventrally; it is delimited by walls formed by the prootic and the opisthotic, and it is bordered medioventrally by the tip of the alary process of the parasphenoid. The walls are not in

contact laterally, leaving an opening (Fig. 4, 3D model 1). The medial tip of the columella is placed in this opening. Thus, it is conceivable that this lateral opening formed the fenestra ovalis, although this fenestra is not limited ventrally by an osseous rim, either because the floor of the otic capsule was cartilaginous, or because the corresponding bone broke off and left no discernible trace. Indeed, a cartilaginous floor would be consistent with other signs (*e.g.* lack of ossification of epiphyses of long bones, see below) that the specimen was not a fully grown adult. The concavity likely housed part of the perilymphatic cistern, which could have had a cartilaginous floor. Indeed, Báez and Nicoli (2004) report a similar condition in *Notobatrachus degiustoi* Reig, 1956 '1955' in Stipaničić and Reig, 1955 (see also Báez, 1996), and Sigurdsen (2008) indicated that the ventrolateral ledge of the opisthotic of anurans houses the posterior part of the perilymphatic cistern. On the left side, the borders of the concavity are less distinct because of the disarticulation of the elements.

A very long crista parotica extends from what we regard as the fenestra ovalis area to the tip of the lateral process of the frontoparietal. There are no indications of an operculum. Each exoccipital forms a posterior sub-triangular bone, to which the occipital condyle is attached. Each exoccipital forms a dorsal protuberance that markedly projects dorsal to the stalk of the occipital condyle (Fig. 6). These dorsal protuberances were illustrated on the figure 2A of RR89, where they are labelled with a question mark (direct examination of the fossil or casts does not show that these protuberances are parts of the exoccipitals). Unfortunately, the articular surfaces of the occipital condyles are barely visible. Post-mortem displacement brought the right thyrohyal against the articular surface of the right condyle. Observation of the contact between the thyrohyal and the condyle suggests that the articular surface of the condyle was not strongly convex, but seemingly flat, similar to the condition seen in *Notobatrachus*, if not as wide and prominently stalked (Báez and Basso, 1996). The foramen magnum is completely indiscernible.

The 'small ovoid bone behind the posterolateral part of the left squamosal' described in RR89 as a possible quadrate can be seen dorsal to the tip of the ramus posterior of the left pterygoid (Fig. 4).

Splanchnocranium

The hyobranchial skeleton is represented by three elements that were originally identified by Piveteau (1937). Ventral to the parasphenoid, a small triradiate element is a parahyoid. Two long elements in the cervical region are probably thyrohyals. They are slightly curved, and wider at the extremes, with flat anterior faces. One of these elements is anteroposterorly oriented, and placed in contact with the right occipital condyle (Fig. 4). The other one is situated between the region where the foramen magnum would be expected to be and the atlantal cotyles (Figs. 4, 6).

The medial parts of the columellae (stapes) are preserved; they are conical and their medial faces have a central depression but they lack a visible notch (RR89). Their medial faces (the 'footplates', pars interna plectri) face ventrally, indicating that they have rotated from their anatomical position.

Axial skeleton

The vertebral column of *Triadobatrachus* comprises at least 26 vertebrae, which are distributed in three regions (Fig. 3). The presacral region corresponds to the 15 vertebrae between the occiput and the sacral region, not 14 as previously reported in RR89 (see below). The sacral region comprises a single sacral vertebra. The caudal region comprises all the vertebrae that are posterior to the sacral vertebra, forming the 'tail' of the animal. The fossil preserves at least 10 caudal vertebrae that decrease in size posteriorly.

Most of the vertebral column is situated in the plane of the fracture of the nodule (Fig. 2), except the last four (or five) caudal vertebrae, which lie in a more dorsal position. The vertebral column is relatively straight from the atlas to the presacral XIII, but it bends slightly (~15º) to the left beginning from the presacral XIV. The vertebrae posterior to the presacral III become incrementally rotated counter-clockwise around the axis of the vertebral column. Most of the ribs are disarticulated and have migrated vertically to the level of the plane of the fracture of the nodule. The presacral ribs are well preserved in the cervico-scapular region, but posterior to that, their preservation is very poor and their length cannot be estimated. Their tips may have been cartilaginous. Note that their reconstitution on the 3D visualisations is very tentative; we intend to give an idea of their position more than a precise estimate of their size and shape.

The general morphology of the vertebrae of *Triadobatrachus* is simple. The centra are cylindrical and biconcave (amphicoelous). The dorsal portion of the neural arch is robust, not very high and has a slightly

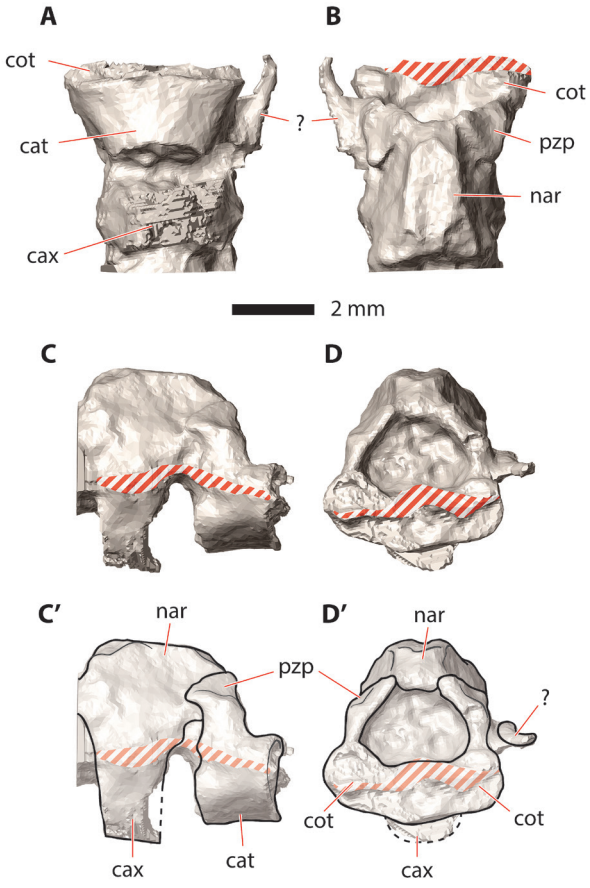

Fig. 7. Visualisations of the atlas-axis complex in ventral (A), dorsal (B), right lateral (C), and frontal (D) views, and interpretative drawings of the last two views (C' and D', respectively). The rough texture of the ventral part of the centrum in ventral view corresponds to a low-density region in the nodule matrix that was segmented manually. The red-white stripe pattern is used to shade areas where the anatomical structures were not preserved in one of the views. The dashed lines in the drawings indicate reconstructed parts. cat, atlantal centrum; cax, centrum of the axis; cot, cotyle; nar, neural arch of the axis; pzp, postzygapophysis of the atlas; ?, element of unknown identity previously identified as a rib.

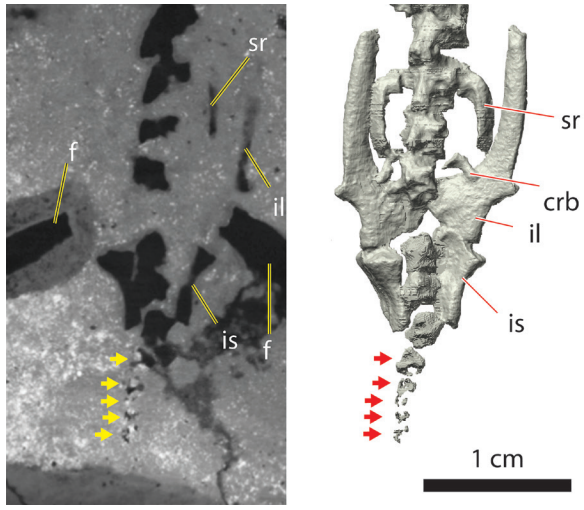

Fig. 8. Tomogram (left) and dorsal view of the 3D model (right) showing the pelvic girdle, the sacral vertebra and the caudal vertebrae. There are 10 or 11 caudal vertebrae; the number of terminal elements is unclear. The arrows in both images indicate caudal vertebrae VI to X (or XI). crb, caudal rib; f, femur; il, ilium; is, ischium; sr, sacral rib.

slanting lateral profile. The posterior part of the neural arch is very thick; it projects posteriorly and overlaps the anterior part of the following vertebra. In terms used in anuran anatomy, the neural arch is of the imbricate type. The dorsal portion of the neural arch has three low longitudinal ridges: an easily discernible sagittal ridge, which is a poorly developed neural spine, and two lateral ridges, which are not always evident. All three ridges extend up to the posterior part of the neural arch. The transverse processes always project laterally, and their articular surfaces are oval. Prezygapophyses and postzygapophyses are present, but the latter are not marked off from the posterior part of the neural arch. The notochordal canal might have remained open, but it is obscured by the type of preservation. It is clear that the notochordal canal remained open at least in the last caudal vertebrae (Fig. 8).

Presacral region

On the casts, a single incomplete neural arch in dorsal view appears in association with the first two vertebral centra visible in ventral view. RR89 interpreted this as the presence of a single atlas with a centrum comprised of two parts. A lateral view of 3D model 1 reveals that in fact these elements correspond to two distinct vertebrae: a small atlas with a dorsoventrally flattened centrum and a dorsally open neural arch comprising only the pedicels, and an axis with a very robust neural arch (Fig. 7). The atlas is in very close contact with the axis by the zygapophyseal articulation. The neural arch of the atlas bears small postzygapophyses on its posterior margin; there is no dorsal osseous neural lamina, *i.e.* no bony roof. There are no indications of transverse processes on the atlas. The neural arch of the axis projects anteriorly; it inserts between the pedicels of the atlas and thus compensates for the absence of the roof of the

atlantal neural arch. The lack of bony neural lamina is a normal feature of immature anurans, in which the neural arch has a cartilaginous roof instead. In the case of the atlas of *Triadobatrachus*, the cartilaginous roof, if present, would be limited to the most anterior part of the neural arch of the atlas only, as the anterior projection of neural lamina of the axis roofs most of the neural arch of the atlas already.

The small articular surfaces between the postzygapophyses of the atlas, formed by the posterior edges of the pedicels, and the prezygapophyses of the axis are visible in lateral view, mainly on the right side. RR89 misinterpreted the dorsal areas of the atlantal postzygapophyses as 'small distinct areas that took part in the craniovertebral articulation'; the 3D renderings show that there is nothing in the occiput that could have participated in such an articulation (3D model 1, Fig. 4).

In ventral view, the centrum of the atlas has roughly the shape of an isosceles trapezium, with the anterior face being the widest. The surface of the anterior face of the atlas is difficult to interpret because the gap left by the fracture of the nodule is wide in this region. The dorsolateral parts of both atlantal cotyles are well preserved but their ventromedial areas are poorly discernible, because the limits are either damaged (right cotyle) or concealed by elements that are likely artefacts (left cotyle). The cotyles are somewhat elongate; their main axes are oblique and seemingly confluent with the main body of the centrum. Apparently, their surfaces are only slightly concave, which is consistent with the observed morphology of the occipital condyles. The ventral border of the anterior face of the centrum slightly protrudes anteriorly in the sagittal plane. It is not possible to state whether the protruding part results from the juxtaposition of the two cotylar rims or if it is formed by the main body of the centrum (the cotyles being separated). The first case would resemble the Type IIIA cotylar configuration of Púgener (2002), albeit with more rounded cotylar faces, whereas the second case would resemble Púgener's cotylar Type IIA, but with more rounded cotylar faces and a significantly higher anterior face of the centrum. Type I, in which the cotyles are widely separated, may be discarded. In any case, it is clear that the atlantal centrum is not as reduced as it is typical of type III atlantes, and that the cotyles do not markedly protrude anterior to the main body of the centrum, unlike the typical condition of lissamphibians.

The ventral part of the axis looks broken upon the examination of casts, but a good part of it has in fact been preserved as a zone of lower density in the matrix, which we were able to recover by manual segmentation (3D model 1). Thus, we confirm that this vertebra was amphicoelous, and that its centrum was at least as high as that of the following vertebrae. The anteroposterior length of the centrum is difficult to determine, as it is evident that the anterior and posterior parts are incomplete; the preserved segment is rather short. As mentioned above, the neural arch is very robust, and wider than that of the following vertebrae. Also, unlike the other vertebrae, the dorsal profile of the neural arch is rather horizontal (as opposed to sloping) in lateral view (Fig. 7). The axis does not show indications of transverse processes either.

Two elements left of the atlas-axis complex and one right to it (Fig. 4), were interpreted as fragments of bicapitate atlantal ribs by RR89. The two left elements were interpreted as fragments of the same rib. The anterior element is long, slender, and slightly curved. The posterior element is longer, also slender, but slightly thicker and bearing a small bifurcation at its anterior end. The right element is markedly shorter, more robust, and has an overall Y-shape. These differences cast doubt on the homology between left and right elements. Furthermore, as visible on the 3D images, the lack of transverse processes or lateral articulations on the first two vertebrae is at odds with the possible presence of ribs in this region. Thus, we question RR89's interpretation of these elements as ribs of the cervical region. They might be parts of the hyobranchial apparatus but this cannot be confirmed.

In the third and fourth presacrals the posterior part of the neural arch is markedly elevated over those of the rest of the presacrals, because the third and fourth vertebrae have been tilted ventrally in the sagittal plane. A small semilunar element is placed anterior to the third presacral, visible in ventral view in the space between the centra II and III. RR89 proposed that it could be a fragment of intervertebral disc, or maybe an articular surface that got detached from the third presacral, the second option implying the third presacral would be opisthocoelous. However, on 3D model 1, the anterior face of the centrum of the third presacral is visible and it is clearly concave. We may propose a third interpretation: the semilunar element could be a fragment of the centrum of the axis. The right rib remains articulated with the transverse process. The left rib has been disarticulated and slightly displaced posteriorly. Both ribs are unicapitate.

The presacral IV (*i.e.*, third vertebra of RR89) was described as 'not very long' by RR89. That could be the case, but the length of the centrum is uncertain, as

its ventral surface is obstructed by the right clavicle, and laterally by the scapulae. On the casts, the posterior part of the neural arch appears damaged and very short, but a good portion of it was preserved in the nodule matrix and could be recovered by manual segmentation. The reconstructed posterior part is longer than may be seen on the casts but it is shorter than in the more posterior vertebrae of the region. It is clear that this vertebra is disarticulated and ventrally tilted in the sagittal plane, as its postzygapophyses are disarticulated from the prezygapophyses of the fifth vertebra (Fig. 4, 3D model 1). The ribs of the fourth vertebra are the longest fully discernible ribs of the skeleton. The neural arch of the presacral V is longer than in more anterior presacrals. From here and to the sacrum, the vertebrae feature roughly the same generalised morphology described above.

Sacral region

The sacral region was already well known. The sacral vertebra is short and its neural arch is narrow. The sacral ribs are robust, long, and curved posteriorwards in such a way that the posterior three quarters of their length are parallel to the anterior rami of the ilia. If that is their natural position, this would indicate a type of sacroiliac attachment that is not known in other salientians.

Caudal region

At least 10 caudal vertebrae are arranged in continuity after the sacrum (Fig. 8). The last four or five of these vertebrae were not previously known. The neural arches of these vertebrae are progressively smaller. After the caudal VI the neural arches are no longer closed dorsally. Distinct transverse processes can be seen up to the caudal V. Yet, a single pair of caudal ribs is visible. As remarked by RR89, it is not possible to determine to which vertebrae they were attached, or if they reached the ilia or sacral ribs laterally.

It is not possible to ascertain to what extent the fragmentary state of the last four or five caudal vertebrae is the result of the fossilisation process, or the reflection of the developmental state of the specimen. The preserved elements seem to be arranged around a tubular structure (now missing). However, whether that structure corresponded to the neural tube or the notochord is not clear, so the aforementioned elements could correspond either to the neural arches or the centra. Furthermore, it is not clear to us whether there are one or two vertebrae after the caudal IX (Fig. 8).

Appendicular skeleton

Shoulder girdle and forelimbs

As noted by RR89, the elements of the shoulder girdle are disarticulated, displaced, and some are broken.

On each side of the vertebral column, a large and flat anterior element, and a smaller and flat posterior element are separated by a gap not much longer than a vertebra in ventral aspect. These elements correspond to the scapula and the coracoid, respectively. They were interpreted as scapula and coracoid (distinct ossifications) by RR89, and as the scapular and coracoidal portions of a single scapulocoracoid bone by Borsuk-Białynicka and Evans (2002).

As seen on the ventral view of the fossil, the preserved part of the right scapula is strikingly anuran-like. More specifically, the dorsal part of the scapular blade (pars suprascapularis) expands anteroposteriorly, whereas the glenoid area does not markedly extend posteriorly. Incidentally, the scapula assigned to *Czatkobatrachus*, the only other known Triassic salientian, seems markedly different in that the preserved portion of its pars suprascapularis is slenderer and features a modest dorsal expansion much more distally (Borsuk-Białynicka and Evans, 2002).

The dorsal tips of both scapulae have rotated laterally, which exposes the medial surfaces of these bones in dorsal view (Fig. 4, 3D model 1), with the elements of the glenoid area exposed ventrally in the region between vertebrae III-VI. The lateral face of the right scapula of *Triadobatrachus* is exposed and the pars suprascapularis, pars acromialis and the anterolateral rim of the glenoid articular facet are clearly apparent. The pars glenoidalis cannot be distinguished. The overall shape of the scapula, with a dorsally expanded pars suprascapularis and a markedly concave anterior border, is similar to that of most anurans. More specifically, it surprisingly matches the elongate morphotype that is not encountered in 'archaeobatrachians' (paraphyletic assemblage comprising Leiopelmatidae, Alytidae, Pipidae, Palaeobatrachidae) (Vullo *et al.*, 2011). There is a furrow along the dorsal margin of the pars suprascapularis, which likely served for the attachment of a cartilaginous suprascapula.

In *Triadobatrachus*, Borsuk-Białynicka and Evans (2002) tentatively identified a supracoracoid foramen on the posterior border of the scapula, and a supraglenoid foramen more dorsally on the same border. In 3D model 1, the former is probably present, and the latter cannot be directly discerned, but the right scapula

does bear a deep vertical cleft similar to the one that houses the supraglenoid foramen in *Czatkobatrachus* (Borsuk-Białynicka and Evans, 2002). The corresponding area is obscured on the left scapula. According to Borsuk-Białynicka and Evans' (2002) interpretation — which was derived from comparisons with *Czatkobatrachus*, — the glenoid area was present somewhere in the gap between the scapular and coracoidal portions, and the distribution of the elements in the fossil specimen derives from the rotation and backward migration of the coracoidal portions. That interpretation is partially supported by two identifications that we could corroborate: the presence of the supracoracoidal foramen, which is topographically close to the glenoid cavity in the plesiomorphic condition of the Anura (Borsuk-Białynicka and Evans, 2002), and the postglenoidal border of the coracoidal portions. However, while those features support the topographical relations proposed by Borsuk-Białynicka and Evans (2002), they do not suffice in our opinion to support the hypothesis that there was a unified scapulocoracoid that got broken into two parts. For example, instead of being co-ossified, the two elements could have been connected by a loose suture, as is frequent in anurans, or by cartilage (Havelková and Roček, 2006).

Ventral to the presacrals III and IV (and V, partially), there are two long parallel elements that probably correspond to the right clavicle broken into two parts. The posterior and smallest of these two elements has been reconstructed in figure 4B; on the casts only a small rounded portion of it is visible. With the addition of this fragment, the reconstituted clavicle is more robust than in RR89 and Borsuk-Białynicka and Evans (2002). Another long element can be found under the left scapula and against the prearticular (Fig. 4); it is probably the left clavicle. The cleithra, flat and long, are slightly displaced but they still overlap the scapulae dorso-anteriorly (Fig. 4).

The forelimbs were described in detail by Sigurdsen *et al*. (2012); here they will be treated more generally. The stylopodia and zeugopodia do not show ossified epiphyses. The humeris is cylindrical and gently sigmoid, with a clear deltopectoral crest. On the distal extremity, the gap between the entepicondyle and the ectepicondyle suggests the presence of a large capitulum (Sigurdsen *et al*., 2012), which was not preserved; it was likely cartilaginous as is the case in salamanders or largely cartilaginous as in the Early Jurassic salientian *Prosalirus*. The radius and the ulna are unfused, and shorter than the humerus. Their transversal sections are oval at the extremities of the bones, and circular at the mid-diaphysis. The ulna is slightly sigmoid. The carpal elements are present on both sides; a proximal row includes the intermedium and probably the radiale and ulnare, whereas a more distal bone represents the central 4 or 3. RR89 observed two distal bones on the casts; they interpreted them as the central 4 and possibly the central 3. However, a single bone is visible on figure 3. No prepollex is visible.

Pelvic girdle and hind limbs

The pelvic girdle has undergone a post-mortem anterior shift with respect to the sacral vertebra and ribs. It is formed by the ilia and the ischia; there are no traces of pubes, which were probably cartilaginous as in most anurans. The two (right and left) halves of the pelvis have been separated and they rotated so that their medial surfaces are now exposed dorsally. The ilium is oriented anteroposteriorly, and bears a dorsal tuber and a long anterior shaft (approximately of the length of the centra of three presacral vertebrae). This anterior shaft does not bear a dorsal crest. As mentioned in RR89, the tip of the anterior shaft is deeply concave (lacking a periosteal surface), suggesting that it was capped or prolonged by cartilage. The acetabulum is clearly visible on the ventral view of the fossil. The ischium is sub-triangular and somewhat elongate anteroposteriorly.

In the reconstruction of RR89, ilia and ischia appear articulated in a fashion typical of anurans, with the two ischia in parasagittal orientation and in full contact between each other by their medial faces. However, the medial face of the ischium is not flat enough to allow that configuration: its anterior region is concave and its posterior region is convex (Fig. 9D). Furthermore, the anterior shaft of the ilium is not as curved as seen in the reconstruction of RR89, making it impossible to accommodate the sacral ribs between them if the medial faces of the ischia were entirely in contact.

From our attempts to make a re-articulation of the basin based on 3D model 1, a feasible range of articulation of the pelvic elements becomes apparent (Fig. 9). It goes from ischia in parasagittal orientation and articulated to each other by a thick pad of connective tissue (Fig. 9B, 3D model 2 in online supplementary information S3), to ischia in ventro-parasagittal orientation and articulated to each other by their ventromedial margins, as seen in caudates (Fig. 9A, 3D model 3 in online supplementary information S4). The orientation of the ilia would vary accordingly. In the first case ('narrow configuration'), the acetabula would be oriented laterally

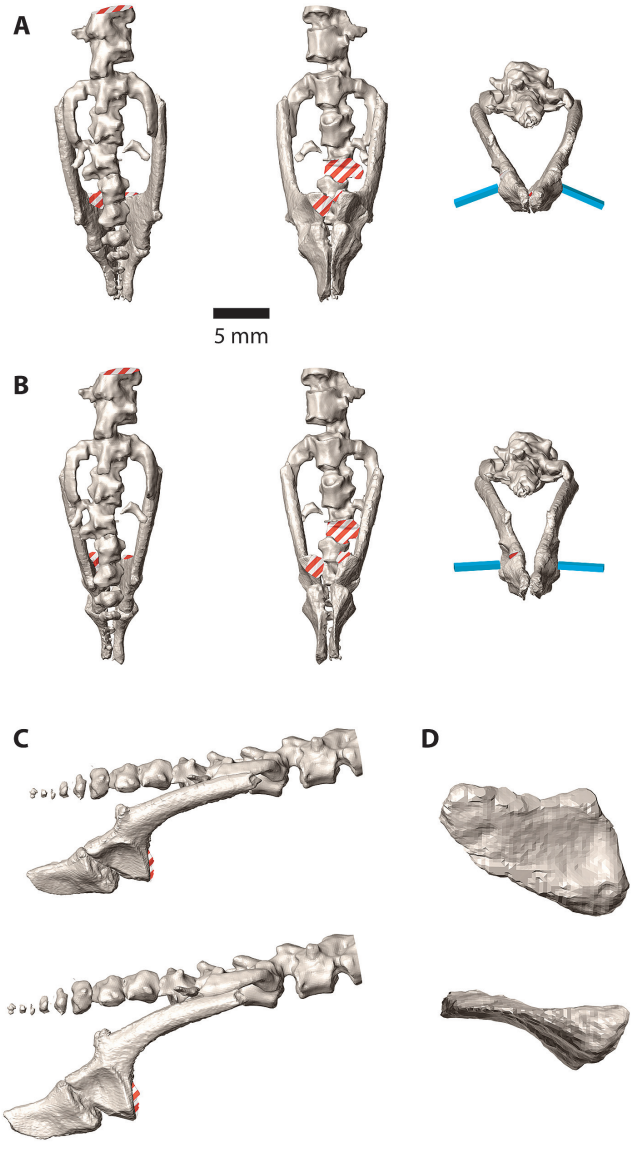

Fig. 9. Reconstructions of the pelvis illustrating a plausible range of articulations of the pelvic bones. A, dorsal, ventral, and posterior views of a 'broad' pelvis reconstruction in which the contact between the ischia is ventromedial (as in caudates) and the sacral ribs can lie mediodorsal to the iliac shafts. In the posterior view the slightly ventral orientation of the acetabulum is shown by blue bars orthogonal to the plane of the rim of the acetabulum. In B, the corresponding views show a 'narrow' pelvis reconstruction where the contact of the ischia is more extensive; in this reconstruction, the space between the iliac shafts is narrower, and the sacral ribs lie completely dorsal to the shafts. As in anurans, the projection of the acetabulum is mostly horizontal. However, unlike in anurans, the contact between the ischia cannot be close, because their medial faces are not flat. C shows lateral right views of the 'broad' (top) and 'narrow' (bottom) reconstructions. The posterior caudal vertebrae have been rearranged for aesthetic purposes, but the vertebral column has not been altered otherwise. The isolated left ischium is shown in D, in medial (top) and ventral (bottom; medial side facing up, lateral side facing down) views. Note the concavity in the anterior region of the medial face of the ischium, visible in medial view, and the convexity of the posterior region of the medial face, visible in ventral view. This prevents full contact between the medial faces of the two ischia. The red-white stripe shading is used to indicate areas where the anatomical structures were not preserved.

and the sacral ribs would likely lie dorsal to the anterior shafts of the ilia. In the latter case ('broad configuration'), the acetabula would face latero-ventrally, and the sacral ribs could lie dorso-medial to the anterior rami of the ilia. Furthermore, the posterior margins of the medial faces of the acetabular areas lack any trace of contact with each other, supporting a loose attachment between the two ilia, as is seen in urodeles (Gardner *et al.*, 2010).

Our re-articulated basin models are also compatible with the presence of a gap between the ilium and the ischium at the ventral margin of the acetabulum (Fig. 9C). That feature is present in anurans, in which it corresponds to the placement of the cartilaginous pubis. However, we should warn that the anterior margin of the ischia and the ventral tips of the pars descendens of the ilia are partially obscured because of overlapping in the fossil, adding uncertainty to the re-articulation models.

The femur is long, slightly sigmoid, and lacks any crests or distinct processes. The proximal epiphysis are not present; they were probably cartilaginous. The

dorsal half of the distal end of the right femur is preserved, and suggests that the distal epiphyses were cartilaginous as well. The zeugopod is shorter than the femur (whereas it is longer or sub-equal in the Anura), and is formed by separate tibiae and fibulae. The right tibia and fibula are almost completely preserved; they are more flat than the femur, especially the tibia. The proximal and distal epiphyses are missing. As in the femora, they were probably cartilaginous. A faint trace of the left tibia is preserved in dorsal view. The four tarsal elements of the right extremity described by RR89 are well exposed; these include the relatively long tibiale and fibulare, the intermedium (displaced and located between the extremities of the tibia and fibula), and the central 4 (displaced too, located against the intermedium). A small portion of the tibiale seems to have been detached. Another possible tarsal element is found left to the fibulare, but only a small fragment of it has been preserved and its shape cannot be clearly ascertained; it may be a central or a metatarsal, if it is a bone at all. There is no evidence of a prehallux.

Ancestral character estimation

Rate shift model selection

We fitted up to six BM rate shift models on trees reflecting the lepospondyl and the temnospondyl hypotheses (see methods section and Figs. 10 and 11), each with branch lengths adjusted to six sets of divergence age estimates (Table 2). The best fit (Akaike weights over 0.99) for the number of presacral vertebrae was obtained under all divergence age sets and under both topologies (LH and TH) with the model with the greatest number of parameters (corresponding to the models with more local rate partitions). The PSL/SW ratio data was best fitted under all divergence age sets and both topologies (LH and TH) by the model with a local rate for the 'short-body' forms (in addition to a background rate), with Akaike weights over 0.72. In all the analyses the single-rate model had very low Akaike weights. We did not fit models including local rates for gymnophionomorphs to our PSL/SW ratio data, because we do not have measurements of this group.

As expected, in all the analyses, salientians show lower relative rates of evolution (under 0.01 times the global rate of the tree), which coincides with their high conservatism of short-trunked proportions and presacral vertebral count. On the other hand, we found that lepospondyls and gymnophionomorphs evolve the number of presacral vertebrae at a rate over an order of magnitude higher than the global rate of evolution of that trait.

Estimation of ancestral number of presacral vertebrae

The estimated number of presacral vertebrae for various nodes is summarised in Table 3 and Figs. 10 and 11. Rounding off to the nearest integer (which is appropriate because vertebrae are discrete elements), caudates and salientians have an estimated ancestral value of 14-15 presacrals (~12-18 taking the 95% confidence intervals into account). (Note that as Caudata and Salientia are sister total-groups, they both share the same ancestral node. For convenience, when we report the ancestral value of a character of a total group, we actually refer to the value corresponding to the first divergence within that total group according to the specific tree under discussion.) The ancestral value of batrachians is of 15 to 16 presacral vertebrae in all the analyses except those assuming the TH and the divergence age sets 4 and 6, which imply the oldest geological ages. In those cases, the estimated value is 19 and 18, respectively. The estimated ancestral number of presacral vertebrae of batrachians under the TH is always greater than the corresponding estimates under the LH. These results are counterintuitive, given that the putative lepospondyl ancestors of lissamphibians would have significantly longer trunks than temnospondyl ancestors. The explanation for this apparent paradox is that our analyses found that trunk length evolves significantly faster in lepospondyls than in most lissamphibians. As high rates of evolution result in branch scaling by big factors (in the range of 49-132), the scaled branch connecting lepospondyls with lissamphibians becomes exceedingly long, diminishing dramatically the influence of lepospondyls in the estimation of the ancestral values of the few most basal lissamphibian nodes. In addition to this, the last common ancestor of *Gerobatrachus* and lissamphibians under the TH is inferred to have been much more recent (mid-Cisuralian, using our settings to time-calibrate the trees) than the last common ancestor of *Brachydectes* and lissamphibians under the LH (mid-Pennsylvanian), because of the geological age of the relevant taxa, and this exacerbates the difference in influence that temnospondyls and lepospondyls have over the ancestral vertebral number for Lissamphibia and Batrachia. *Gerobatrachus* has 17 presacral vertebrae, which is one to three vertebrae fewer than the ancestral estimate for lissamphibians in five out of six of our analyses under the TH. This suggests a small degree of

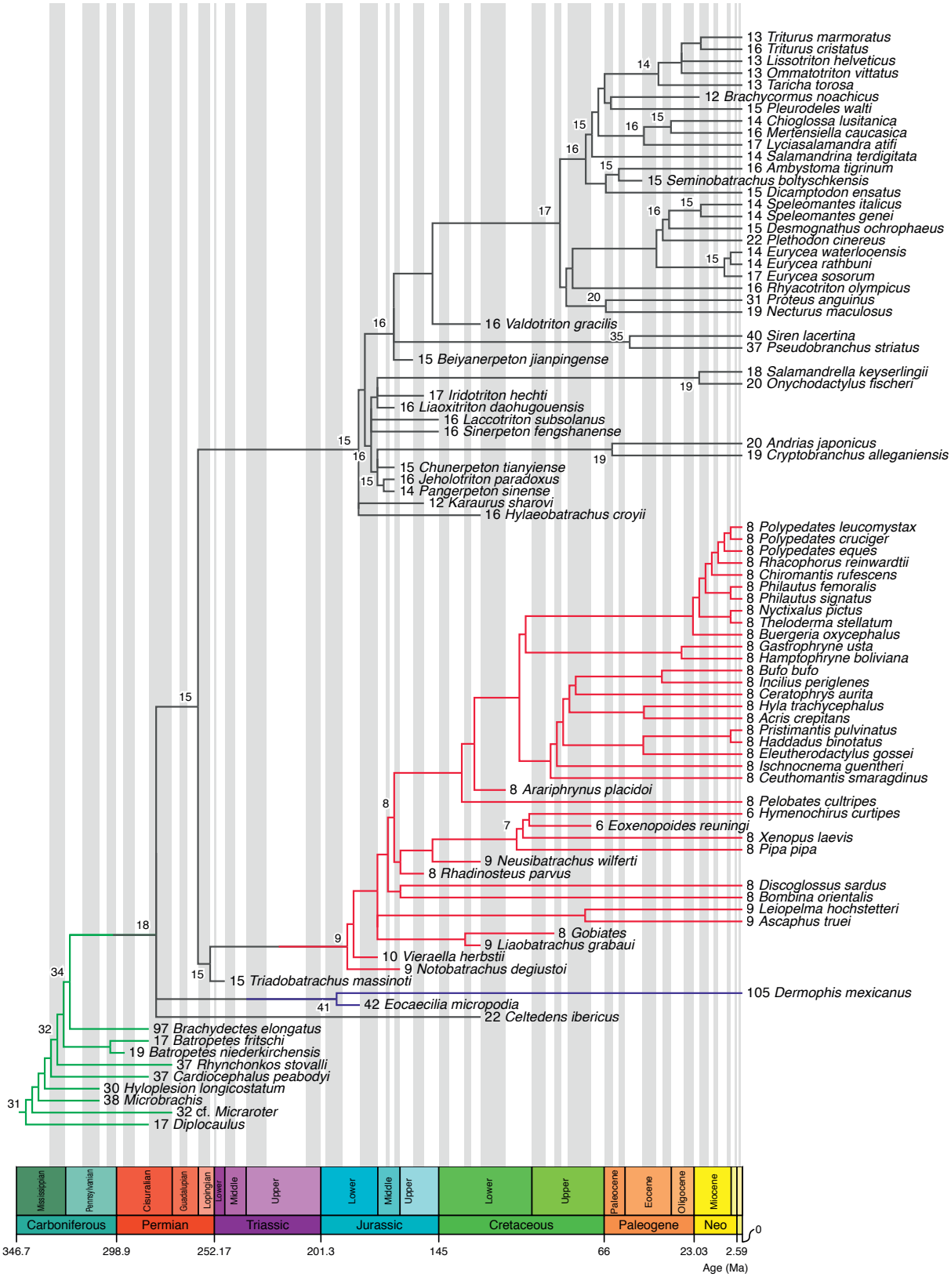
13 Triturus marmoratus
16 Triturus cristatus
13 Lissotriton helveticus
13 Ommatotriton vittatus
13 Taricha torosa
12 Brachycormus noachicus
15 Pleurodeles walti
14 Chioglossa lusitanica
16 Mertensiella caucasica
17 Lyciasalamandra atifi
14 Salamandrina terdigitata
16 Ambystoma tigrinum
15 Seminobatrachus boltyschkensis
15 Dicamptodon ensatus
14 Speleomantes italicus
14 Speleomantes genei
15 Desmognathus ochrophaeus
22 Plethodon cinereus
14 Eurycea waterlooensis
14 Eurycea rathbuni
17 Eurycea sosorum
16 Rhyacotriton olympicus
31 Proteus anguinus
19 Necturus maculosus
16 Valdotriton gracilis
40 Siren lacertina
37 Pseudobranchus striatus
15 Beiyanerpeton jianpingense
18 Salamandrella keyserlingii
20 Onychodactylus fischeri
17 Iridotriton hechti
16 Liaoxitriton daohugouensis
16 Laccotriton subsolanus
16 Sinerpeton fengshanense
20 Andrias japonicus
19 Cryptobranchus alleganiensis
15 Chunerpeton tianyiense
16 Jeholotriton paradoxus
14 Pangerpeton sinense
12 Karaurus sharovi
16 Hylaeobatrachus croyii
8 Polypedates leucomystax
8 Polypedates cruciger
8 Polypedates eques
8 Rhacophorus reinwardtii
8 Chiromantis rufescens
8 Philautus femoralis
8 Philautus signatus
8 Nyctixalus pictus
8 Theloderma stellatum
8 Buergeria oxycephalus
8 Gastrophryne usta
8 Hamptophryne boliviana
8 Bufo bufo
8 Incilius periglenes
8 Ceratophrys aurita
8 Hyla trachycephalus
8 Acris crepitans
8 Pristimantis pulvinatus
8 Haddadus binotatus
8 Eleutherodactylus gossei
8 Ischnocnema guentheri
8 Ceuthomantis smaragdinus
8 Arariphrynus placidoi
8 Pelobates cultripes
6 Hymenochirus curtipes
6 Eoxenopoides reuningi
8 Xenopus laevis
8 Pipa pipa
9 Neusibatrachus wilferti
8 Rhadinosteus parvus
8 Discoglossus sardus
8 Bombina orientalis
9 Leiopelma hochstetteri
9 Ascaphus truei
8 Gobiates
9 Liaobatrachus grabaui
10 Vieraella herbstii
9 Notobatrachus degiustoi
15 Triadobatrachus massinoti
105 Dermophis mexicanus
42 Eocaecilia micropodia
22 Celtedens ibericus
97 Brachydectes elongatus
17 Batropetes fritschi
19 Batropetes niederkirchensis
37 Rhynchonkos stovalli
37 Cardiocephalus peabodyi
30 Hyloplesion longicostatum
38 Microbrachis
32 cf. Micraroter
17 Diplocaulus
Mississippian
Pennsylvanian
Cisuralian
Guadalupian
Lopingian
Lower
Middle
Upper
Lower
Middle
Upper
Lower
Upper
Paleocene
Eocene
Oligocene
Miocene
Carboniferous
Permian
Triassic
Jurassic
Cretaceous
Paleogene
Neo
346.7
298.9
252.17
201.3
145
66
23.03
2.59
0
Age (Ma)

parallel reduction, but also fits nicely within the 95% confidence intervals of those estimates.

The ancestral value estimate for lissamphibians was more variable between topologies and divergence age sets, but they were in all cases equal or up to four vertebrae greater than the ancestral value estimated for batrachians.

The mean estimates of all the analyses, except those done under the divergence age sets 4 and 6, support the hypothesis that the number of presacral vertebrae of *Triadobatrachus* was close to the ancestral condition of caudates and bratrachians, all of these taxa exhibiting a low number of vertebrae apparently resulting from a phase of presacral vertebral number reduction in the early evolution of batrachians. However, as expected, there is extensive overlap of 95% confidence intervals between parent and child nodes.

The ancestral value estimates for the internal nodes of Caudata and Salientia were virtually the same in all the analyses (when rounded off to the nearest integer).

Table 3. Ancestral character estimates of selected nodes. We report the result of ancestral character reconstruction of presacral vertebrae number (A and B) and presacral length/skull width ratio (C and D), using the best-fit models across the six different sets of divergence dates and the two alternative topologies (LH and TH). Note the uniformity of the estimates of salientians and caudates. 95% confidence intervals reported between parentheses. For comparison, the presacral length/skull width ratio of *Triadobatrachus* is about 1.7.

	Set	*Lissamphibia*	*Batrachia*	*Salientia*	*Caudata*
A. NPSV LH	1	16.7 (11.5-21.8)	15 (11.8-18.3)	14.6 (12.2-17)	15.2 (12.7-17.6)
	2	15 (11.7-18.2)	14.8 (12-17.5)	14.5 (12.2-16.9)	15.2 (12.8-17.5)
	3	15.4 (11.4-19.3)	14.7 (12-17.5)	14.5 (12.2-16.8)	15.2 (12.8-17.5)
	4	17.3 (11.3-23.3)	16.4 (11.2-21.6)	14.4 (12-16.8)	15.3 (12.8-17.7)
	5	16.9 (11.1-22.8)	15.1 (11.5-18.6)	14.4 (12.1-16.8)	15.2 (12.8-17.6)
	6	17.9 (11.4-24.4)	16.3 (11.1-21.5)	14.4 (12-16.8)	15.3 (12.8-17.7)
B. NPSV TH	1	18.9 (15.9-21.9)	15.8 (12.7-18.9)	14.9 (12.5-17.4)	15.2 (12.6-17.9)
	2	16.5 (13.5-19.5)	15.8 (13.1-18.6)	15.2 (12.8-17.7)	15.2 (12.5-18)
	3	17.6 (14.6-20.7)	15.7 (12.9-18.5)	15.2 (12.7-17.7)	15.2 (12.5-18)
	4	20.3 (17-23.6)	18.5 (14.3-22.7)	14.7 (12.1-17.3)	15.4 (12.7-18)
	5	19.7 (16.4-22.9)	15.9 (12.4-19.4)	14.8 (12.3-17.2)	15.2 (12.6-17.8)
	6	20.3 (17.1-23.5)	17.7 (13.4-21.9)	14.6 (12.2-17)	15.3 (12.9-17.8)
C. PL/SW LH	1	2.9 (0.9-4.8)	2.1 (0.7-3.5)	1.8 (0.8-2.9)	2.3 (1.2-3.4)
	2	2.2 (0.7-3.6)	2 (0.8-3.3)	1.9 (0.8-3)	2.3 (1.2-3.4)
	3	2.4 (0.8-4.1)	2 (0.8-3.3)	1.9 (0.8-2.9)	2.3 (1.2-3.4)
	4	3.4 (1.6-5.3)	2.9 (1-4.9)	1.8 (0.7-2.9)	2.3 (1.2-3.4)
	5	3.2 (1.2-5.3)	2.2 (0.6-3.7)	1.8 (0.7-2.9)	2.3 (1.2-3.4)
	6	3.7 (1.9-5.5)	2.8 (0.8-4.9)	1.8 (0.6-2.9)	2.3 (1.2-3.5)
D. PL/SW TH	1	2.1 (0.8-3.3)	1.8 (0.6-3)	1.7 (0.8-2.6)	2.3 (1.3-3.3)
	2	1.9 (0.7-3.1)	1.9 (0.8-2.9)	1.8 (0.8-2.7)	2.3 (1.3-3.3)
	3	2 (0.7-3.4)	1.8 (0.8-2.9)	1.7 (0.8-2.7)	2.3 (1.3-3.2)
	4	2.1 (0.8-3.4)	2 (0.4-3.6)	1.7 (0.7-2.6)	2.3 (1.3-3.3)
	5	2.1 (0.8-3.4)	1.8 (0.5-3.2)	1.7 (0.7-2.6)	2.3 (1.3-3.3)
	6	2.1 (0.8-3.5)	2 (0.3-3.7)	1.6 (0.7-2.6)	2.3 (1.3-3.3)

◀ *Fig. 10*. Ancestral value estimations of the number of presacral vertebrae under LH and set 1 of divergence date estimates. Numbers at the terminal items indicate the observed number of presacral vertebrae. Numbers next to the internal nodes indicate the inferred number or presacral vertebrae, with decimals rounded-off. Internal nodes without a number have the same value as their parent node. The colours indicate the regions of the tree with different rates of evolution of the trait. The region with the global rate is in grey, the region with the rate of gymnophionomorphs is in blue, the region with the rate of lepospondyls is in green, and the region with the rate of 'short-body' forms (salientians excluding *Triadobatrachus*) is in red. The tree is taken from the literature, from several sources: extinct lissamphibians follow Marjanović and Laurin (2014); lepospondyls follow Vallin and Laurin (2004). Taxonomic sampling reflects to a large extent availability of the data (some clades, such as sooglossids, could not be included because we lacked the required data).

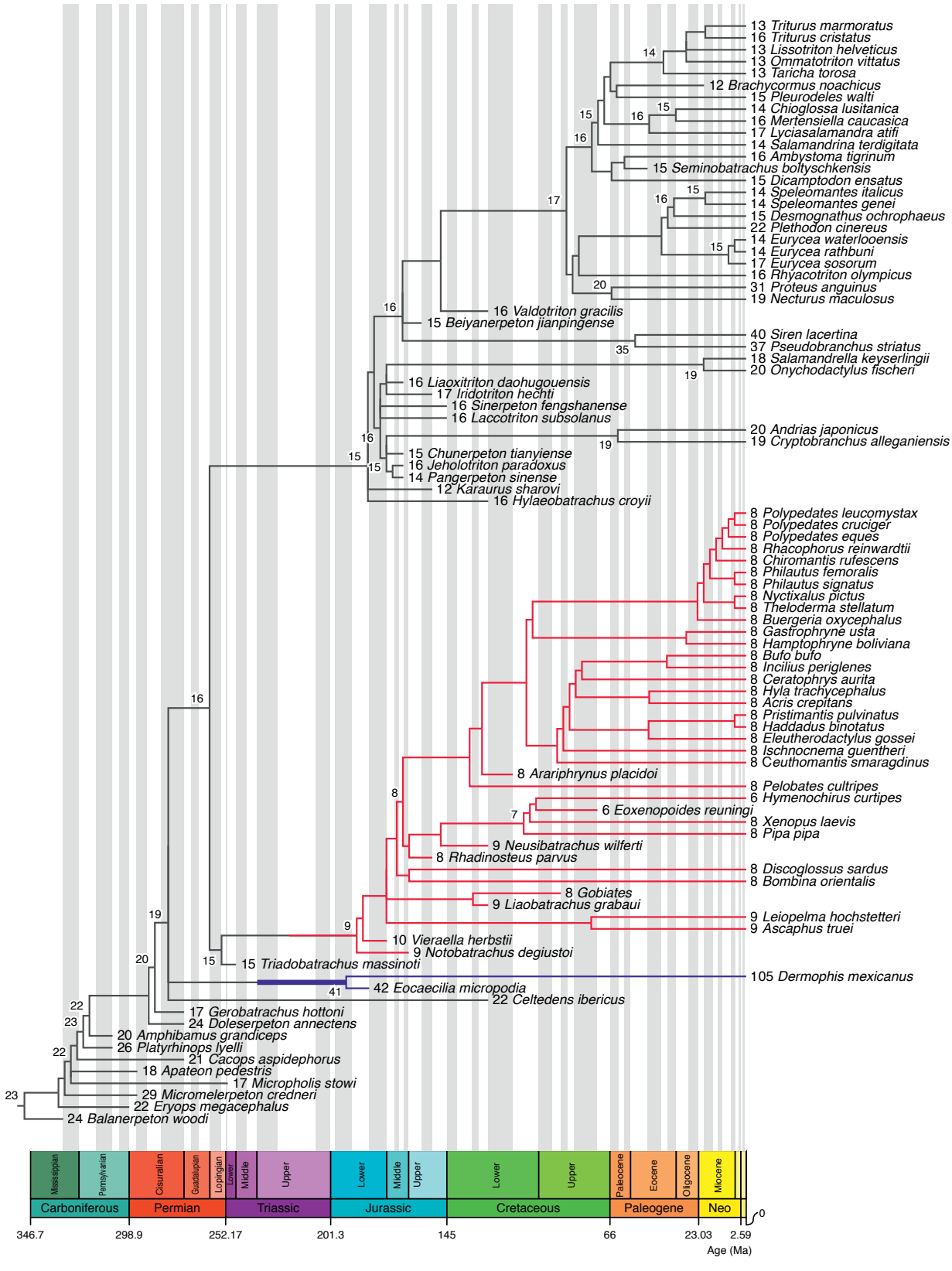
13 Triturus marmoratus
16 Triturus cristatus
13 Lissotriton helveticus
13 Ommatotriton vittatus
13 Taricha torosa
12 Brachycormus noachicus
15 Pleurodeles walti
14 Chioglossa lusitanica
16 Mertensiella caucasica
17 Lyciasalamandra atifi
14 Salamandrina terdigitata
16 Ambystoma tigrinum
15 Seminobatrachus boltyschkensis
15 Dicamptodon ensatus
14 Speleomantes italicus
14 Speleomantes genei
15 Desmognathus ochrophaeus
22 Plethodon cinereus
14 Eurycea waterlooensis
14 Eurycea rathbuni
17 Eurycea sosorum
16 Rhyacotriton olympicus
31 Proteus anguinus
19 Necturus maculosus
16 Valdotriton gracilis
15 Beiyanerpeton jianpingense
40 Siren lacertina
37 Pseudobranchus striatus
18 Salamandrella keyserlingii
20 Onychodactylus fischeri
16 Liaoxitriton daohugouensis
17 Iridotriton hechti
16 Sinerpeton fengshanense
16 Laccotriton subsolanus
20 Andrias japonicus
19 Cryptobranchus alleganiensis
15 Chunerpeton tianyiense
16 Jeholotriton paradoxus
14 Pangerpeton sinense
12 Karaurus sharovi
16 Hylaeobatrachus croyii
8 Polypedates leucomystax
8 Polypedates cruciger
8 Polypedates eques
8 Rhacophorus reinwardtii
8 Chiromantis rufescens
8 Philautus femoralis
8 Philautus signatus
8 Nyctixalus pictus
8 Theloderma stellatum
8 Buergeria oxycephalus
8 Gastrophryne usta
8 Hamptophryne boliviana
8 Bufo bufo
8 Incilius periglenes
8 Ceratophrys aurita
8 Hyla trachycephalus
8 Acris crepitans
8 Pristimantis pulvinatus
8 Haddadus binotatus
8 Eleutherodactylus gossei
8 Ischnocnema guentheri
8 Ceuthomantis smaragdinus
8 Arariphrynus placidoi
8 Pelobates cultripes
6 Hymenochirus curtipes
6 Eoxenopoides reuningi
8 Xenopus laevis
8 Pipa pipa
9 Neusibatrachus wilferti
8 Rhadinosteus parvus
8 Discoglossus sardus
8 Bombina orientalis
8 Gobiates
9 Liaobatrachus grabaui
9 Leiopelma hochstetteri
9 Ascaphus truei
10 Vieraella herbstii
9 Notobatrachus degiustoi
15 Triadobatrachus massinoti
105 Dermophis mexicanus
42 Eocaecilia micropodia
22 Celtedens ibericus
17 Gerobatrachus hottoni
24 Doleserpeton annectens
20 Amphibamus grandiceps
26 Platyrhinops lyelli
21 Cacops aspidephorus
18 Apateon pedestris
17 Micropholis stowi
29 Micromelerpeton credneri
22 Eryops megacephalus
24 Balanerpeton woodi
Mississippian
Pennsylvanian
Cisuralian
Guadalupian
Lopingian
Lower
Middle
Upper
Lower
Middle
Upper
Lower
Upper
Paleocene
Eocene
Oligocene
Miocene
Carboniferous
Permian
Triassic
Jurassic
Cretaceous
Paleogene
Neo
0
346.7
298.9
252.17
201.3
145
66
23.03
2.59
Age (Ma)

Estimation of ancestral presacral length/skull width ratio

The ancestral value reconstructions of the presacral vertebral length/skull width ratio of caudates are close to 2.3 in all the analyses (Table 3). The corresponding values for salientians are slightly lower under TH (~1.7) than LH (1.8 - 1.9). The ancestral value for batrachians is more variable, ranging from 1.8 to 2.9. The estimates of the ancestral values of salientians range from 95% to 62% of the corresponding ancestral condition of batrachians, the lowest value being obtained under LH and divergence age sets 4 and 6. However, the other divergence age sets suggest that during early salientian evolution the relative trunk length was either unaltered or only moderately reduced (by no more than 15%, compared to the over 50% of Anura). This degree of reduction (to a mean ratio of 1.7-1.9) does not seem to require a particular explanation because more drastic reduction is observed in other early lissamphibians, such as the Jurassic caudate *Karaurus sharovi* Ivakhnenko, 1978 (presacral length/skull width ratio of 1.3). As with the reconstruction of the number of presacral vertebrae, there is extensive overlap between the 95% confidence intervals of all the focal ancestral estimates.

An opposite trend is observed in the estimates of the ancestral condition of caudates, which range from being 1.1 to 1.3 times greater than the corresponding ancestral batrachian condition, except for the LH estimate under the divergence sets 4 and 6, under which the estimated value is about 0.8 times smaller. The ancestral value estimates for batrachians were in all cases smaller than the ancestral estimates for lissamphibians.

As seen in the reconstruction of the number of presacral vertebrae, the ancestral value estimates of nodes crownward from Batrachia were virtually identical between all analyses.

Discussion

An overall picture of our re-interpretation of *Triadobatrachus* is given in Fig. 12. Our major new anatomical findings can be summarised in the following list.

1) Presence of either mentomeckelians or a lingual process of the dentary similar to that found in some temnospondyls.
2) Possible presence of a discrete angular.
3) Presence of dorsal protuberances of the exoccipital.
4) Confirmation of the presence of a ventrolateral ledge of the opisthotic.
5) What was previously identified as an atlas with a double centrum actually corresponds to two distinct vertebrae: atlas and axis.
6) The atlas does not bear a bony roof (neural lamina), but its neural arch is partially completed by an anterior expansion of the neural arch of the axis.
7) There are no transverse processes on the atlas and axis. Hence, the 'cervical ribs' reported in RR89 were misidentified.
8) Weak contact between the two ilia (plesiomorphic relative to anurans).
9) Absence of complete contact between the medial faces of the two ischia.
10) Four or five previously unreported additional caudal vertebrae.
11) From (5) and (10), the updated vertebral formula of *Triadobatrachus* is 15 presacrals, 1 sacral, 10 or 11 caudals.

The particular findings on the craniocervical and caudopelvic regions merit more detailed discussion.

Craniocervical region

The interpretation of the craniocervical region we offer here shows major departures from RR89's. The atlas does not have a bipartite centrum, and it does not bear cervical ribs (the homology of the structures previously identified as cervical ribs remains undetermined, although they could belong to the hyoid apparatus). In our examination, the craniocervical region shows other peculiar features instead.

The vertebral column of tetrapods is characterised by the differentiation of the vertebrae involved in the craniocervical articulation. The atlas is universally differentiated within the group; it bears the cotyle that

◀ *Fig. 11.* Ancestral value estimations of the number of presacral vertebrae under TH and set 1 of divergence data estimates. As in Fig. 10, numbers at the terminal items indicate the observed number of presacral vertebrate. Numbers next to internal node indicate the inferred number of presacral vertebrae, rounded-off to the nearest unit. Internal nodes without a number have the same value as their parent node. The colours indicate the regions of the tree with different rates of evolution of the trait. The region with the global rate is in grey, the region with the rate of gymnophionomorphs is in blue, and the region with the rate of 'short-body' forms (salientians excluding *Triadobatrachus*) is in red. Temnospondyl phylogeny reflects Schoch (2013). For more information, see the legend of Fig. 10.

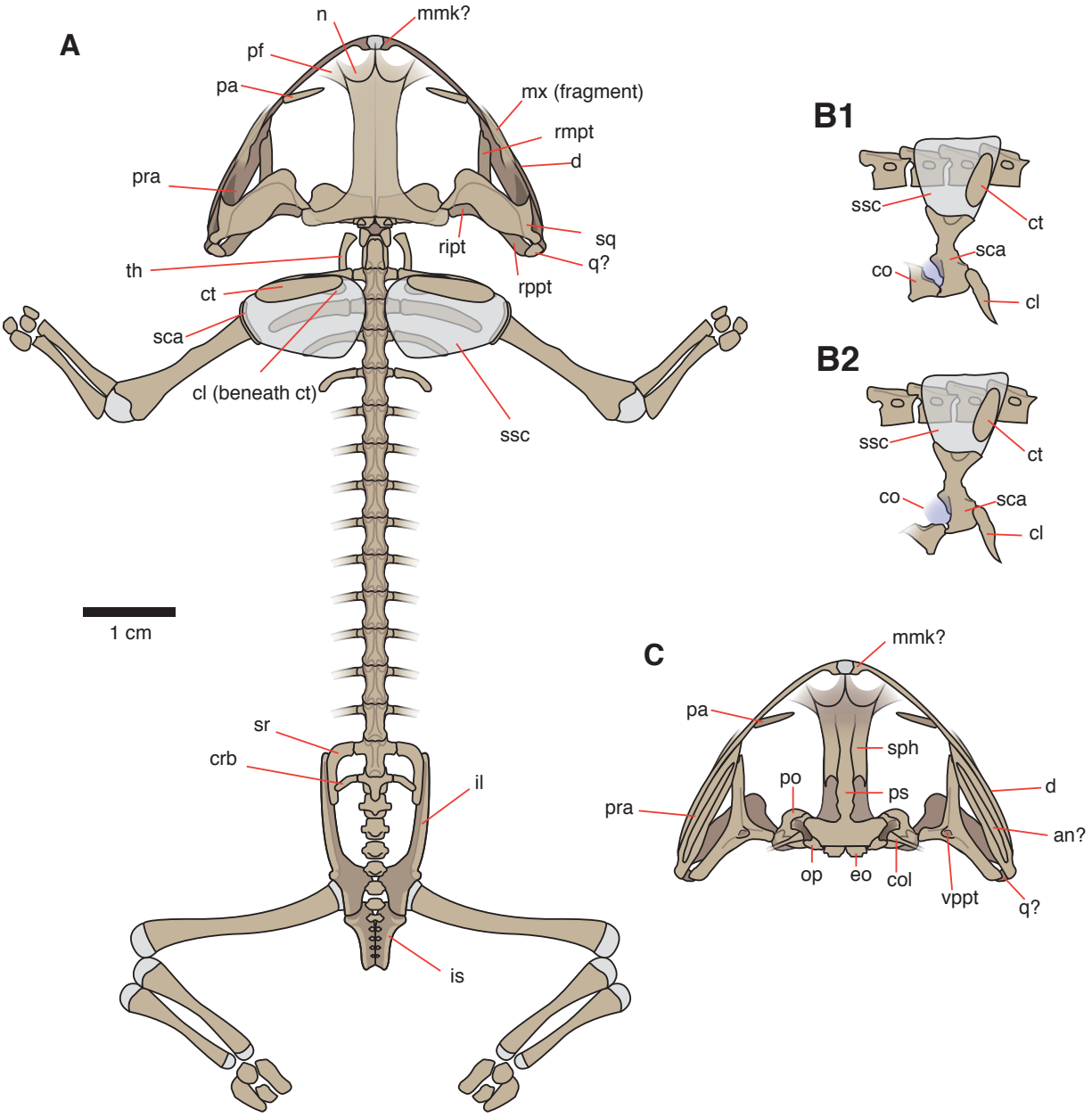

Fig. 12. Interpretative reconstructions of the skeleton of *Triadobatrachus massinoti* in dorsal view (A), the two possible articulations of the right pectoral girdle in lateral view (B), and the skull in ventral view (C). A few cartilages have been reconstructed (in grey) for illustration purposes only; the actual size and shape of the suprascapula is unknown. The position and orientation of the clavicle and the cleithrum are uncertain. This reconstruction features a 'broad' pelvis, with the contact between the ischia limited to their ventral margins, and the sacral ribs resting mostly between the iliac shafts. The pectoral girdle reconstruction B1 features a compact configuration similar to that of *Czatkobatrachus* (Borsuk-Białynicka and Evans, 2002), in which the glenoid is oriented more laterally. Reconstruction B2 features a configuration closer to that of extant anurans. Note that a hypothetical stylar process has been added to the columellae, and that we made no attempt to reconstruct the ventromedial process of the pterygoid, as we have no anatomical equivalents in other amphibians to base a reconstruction upon. an, angular; cl, clavicle; co, coracoid or coracoidal part of the scapulocoracoid; crb, caudal rib; ct, cleithrum; d, dentary; eo, exoccipital; il, ilium; is, ischium; mmk?, mentomeckelian or lingual process; mx, maxilla; n, nasal; op, opisthotic; pa, palatine; pf, prefrontal; po, prootic; pra, prearticular; ps, parasphenoid; ript, internal ramus of the pterygoid; rmpt, maxillary ramus of the pterygoid; rppt, posterior ramus of the pterygoid; sca, scapula or scapular part of the scapulocoracoid; ssc, suprascapula; sph, sphenethmoid; sr, sacral rib; th, thyrohyal; q, ?quadrate; vppt, ventral process of the pterygoid.

articulates with the occipital condyle. The differentiation of the tetrapod axis is more variable in type and degree, but it often features a large neural spine and a special articulation with the atlas. In batrachians, however, this kind of differentiation of the second vertebra is virtually absent. *Triadobatrachus* is an exception here, as atlas and axis form a complex in which the anteriorly expanded neural spine of the axis roofs the otherwise dorsally open neural arch of the atlas. We are unaware of previous reports of the axial spine roofing the atlantal arch in other vertebrates, even though the atlantal arch is paired and the axial arch is expanded in many Permo-Carboniferous stegocephalians, and that the lack of a bony neural lamina is a common feature of immature anurans. The condition in *Triadobatrachus* may have arisen through an anterior expansion of the axial arch, from a fairly primitive stegocephalian condition.

The atlas-axis configuration of *Triadobatrachus* could be either autapomorphic or ancestral to salientians, and maybe batrachians. New fossil findings are needed to assess its phylogenetic significance.

Another peculiarity of *Triadobatrachus* among salientians is the presence of a dorsal protuberance of the exoccipital. We were unable to find clear homologues or even analogues of this structure in other lissamphibians or in Paleozoic tetrapods. There is the possibility that this structure did not in fact protrude on the external surface of the skull, for instance, if the exoccipital was more robust than the surrounding bones and was pushed out as the skull was crushed into the horizontal plane. Evidence exists of the compression of the left side of the skull (Fig. 6A), and the left exoccipital has clearly rotated towards the horizontal plane, as the surface of its condyle is not in the same plane as the surface of the right condyle (which seems well-positioned for the articulation with the atlantal cotyle). We find, however, no clear indications of displacement of the right exoccipital. Sadly, the medial region of the occiput of *Triadobatrachus* is poorly preserved. If this external protuberance was not an artefact, its role, if any, remains enigmatic and possibly autapomorphic.

Caudopelvic region

We have shown that some features of the pelvic girdle of *Triadobatrachus* were probably more primitive than previously assumed. The contact between both ischia was not as close as in anurans, and the posterior parts of the ilia were probably even further apart from each other than in anurans. It is likely that the pelvis of *Triadobatrachus* was more loosely built than the specialised compact unit of anurans. Moreover, if the arrangement of the pelvic bones was closer to our reconstructed 'broad configuration', the orientation of ilia and ischia in the transversal plane would resemble the plesiomorphic condition of tetrapods, as seen in salamanders. Correspondingly, the orientation of the hind limbs would likely not be completely horizontal as it is common in anurans, but with a distinct ventral component.

It should be noted that as the fossil has been flattened, there is also uncertainty in the inclination of the pelvic girdle relative to the body axis. Our reconstructions were based on the position of the sacral ribs as seen in the fossil, and thus the anterior shaft of the ilium descends at an angle of about 30º. This angle is often greater in adult anurans, and more so in early ontogeny (Ročková and Roček, 2005).

In contrast to those seemingly more plesiomorphic traits, there is no trace of the pubis of *Triadobatrachus*, whereas an ossified pubis is regarded as plesiomorphic within the Anura, as it is present in *Ascaphus*, *Leiopelma*, and pipids (Ročková and Roček, 2005). The lack of ossified pubis in *Triadobatrachus* could be homoplastic, or a consequence of the state of maturity of the specimen.

The caudal region of *Triadobatrachus* has long been thought to have had more vertebrae than were apparent by direct observation of the fossil (*e.g.* RR89). Here we reported the first evidence of that. The size and shape of the most posterior vertebrae seen in the specimen are concordant with what could be expected of the actual terminal or sub-terminal vertebrae; it is likely that what we report here is the entire, or almost entire caudal region of *Triadobatrachus*. Such a caudal region may not have protruded posterior to the ischia and may thus not have been visible externally (*i.e.*, *Triadobatrachus* would have lacked a 'proper' tail), contrary to previous depictions in the technical (*e.g.* RR89: fig. 5) and popular literature. However, this cannot be regarded as certain.

If one assumes that the last caudal elements are mostly well-preserved, then these somewhat resemble the caudal vertebrae of the tadpoles of several megophryid species, which are resorbed during metamorphosis as most recently described in detail by Handrigan and Wassersug (2007b). Indeed, Griffiths (1956; 1963) argued that the caudal vertebrae of *Triadobatrachus* were to be resorbed, as seen in the development of *Megophrys major* (Boulenger, 1908), concordantly with his hypothesis that the holotype of

Triadobatrachus was a late metamorph rather than in a later ontogenetic stage. Accordingly, the moderately elongated ilia and the proportions of the limbs would reflect an early developmental stage rather than primitive character states.

If our new observations are taken to support Griffiths' analogy between the caudal portions of *Triadobatrachus* and *Megophrys* larvae, the interpretation of *Triadobatrachus* as a late metamorph remains problematic. RR89 disputed it by pointing out several features in *Triadobatrachus* that are observed in post-metamorphic anurans: full development of skull bones, columella of adult proportions, and presence of ossified parahyoid and thyrohyals. The hypothesis of the resorbing tail can still be reconciled with the interpretation of *Triadobatrachus* being a post-metamorphic juvenile, simply by positing that *Triadobatrachus* did not undergo complete resorption of its caudal vertebrae, and that the remnants observed persisted in the adult form, or that this resorption occurred a bit later in ontogeny. In this scenario, the process of caudal vertebrae resorption would have been displaced earlier in ontogeny (through heterochrony) in the subsequent evolution of salientians.

Jumping capacity in Triadobatrachus

The musculoskeletal system of terrestrial tetrapods results from adaptation for locomotion in their environment. Thus, in the trophic interactions of tetrapods, *i.e.* predation or predator avoidance, their mode of locomotion depends on the physical and geometrical structure of the environment. For example, in arboreal environments, individuals must walk, run or jump in the trees and between branches for escape. Thus, the analyses of phenotypic traits like skeletal morphology could yield clues about the usual mode of locomotion of extinct taxa, such as *Triadobatrachus*, and consequently their environment. In extant anurans, one aquatic and two terrestrial (jumpers and walker-hoppers) locomotor behaviours are classically considered. As a further refinement of the terrestrial categories, Enriquez-Urzelai *et al.* (2015) recognised four subgroups. Jumpers were divided into terrestrial (TJ – Terrestrial Jumpers) and arboreal species which climb extensively (AJ – Arboreal Jumpers). Fossorial species that burrow with the posterior extremities were separated from Walkers-Hoppers (WH) and qualified as Burrower-Walker-Hoppers (BWH). In anurans, aquatic locomotion is highly stereotyped with a simultaneous extension of the hindlimbs, even if differences in the inter-articular coordination of the hindlimb joints can be found between some clades (Nauwelearts *et al.*, 2005; Richards, 2010). Aquatic locomotion will not be discussed further here, as there are no indications of *Triadobatrachus* being specialised for swimming (contra Griffiths, 1963).

One of the main issues in the literature concerning the locomotion of *Triadobatrachus* is its ability to jump (*e.g.* RR89; Sigurdsen *et al.*, 2012). Morphology of the trunk, the caudal vertebrae, the fore- and the hind limbs led some previous authors to postulate that *Triadobatrachus* was built for lateral undulatory walking (Reilly and Jorgensen, 2011) and that saltatory locomotion was incipient (RR89). However, an analysis of the forelimbs and pectoral girdle led Sigurdsen *et al.* (2012) to suggest that jumping or hopping was part of *Triadobatrachus,* locomotor repertoire.

Jumping is defined as a leap in which the animal is initially stationary (McNeill, 2003). Its impulse is produced by simultaneous extension of the hindlimbs, and landing occurs on the forelimbs in anurans (*e.g. Pelophylax* kl. *esculentus*; Nauwelaerts and Aerts, 2006). Thus, jumping capacity depends on the ability of the hindlimb extensors to produce maximal power output during a stretch-shortening cycle (McNeill and Bennet-Clark, 1977), and the forelimb extensors to absorb mechanical energy through eccentric contraction (Nauwelaerts and Aerts, 2006, Legreneur *et al.*, 2012a).

It is clear that the musculo-skeletal architecture of forelimbs allowed *Triadobatrachus* to absorb a certain part of mechanical energy at landing, as suggested by Sigurdsen *et al.* (2012). However, the short lengths of the humerus, radius, and ulna imply the use of another damping mechanism, *i.e.* energy absorption by the trunk that would follow the flexion of the forelimbs. One mechanism could be the form of the pectoral girdle structure, *i.e.* arciferal *vs.* firmisternal. The latter would be less efficient in landing because arciferal girdle would allow the animal to decelerate over a greater distance through rotation of the scapula (Emerson, 1983, 1988). However, a biomechanical interpretation of the arciferal girdle as a shock absorption mechanism is not convincing since the firmisternal structure appears only in more recent anuran groups. Moreover, the arciferal girdle is found in anurans belonging to many locomotor categories, such as AJ (Hylidae), WH (Bufonidae), TJ (Discoglossidae, also called Alytidae or Bombinatoridae in the recent literature, and Pelodytidae), and BWH (Pelobatidae). In *Triadobatrachus*, the pectoral girdle is very poorly preserved. However, given that *Triado-*

batrachus represents an early salientian, and because of the curved shape of its clavicle (RR89), we can assume that the girdle was not firmisternal. Borsuk-Białynicka and Evans' (2002) reconstruction of the scapula and coracoid of *Triadobatrachus*, like our own reconstruction, suggests that it would not be arciferal either. Another damping mechanism would involve the cartilaginous suprascapula. In *Triadobatrachus*, the suprascapula is not preserved. We can therefore suppose that it was mainly cartilaginous and maintained by the furrow on the dorsal margin of the scapula. Given these data, it seems that the musculoskeletal structure of the forelimbs and pectoral girdle would have been able to damp the forces generated by landing after a free fall phase. However, unlike Sigurdsen *et al*. (2012), we do not consider that this condition alone suffices to infer that *Triadobatrachus* was able to jump. Before landing, it is necessary to take off.

Jumping impulsion is organized into two distinct phases (Legreneur *et al*., 2010). First, an extension of the forelimbs orientates the body's centre of mass velocity vector (Emerson and De Jong, 1980). This orientation is close to 45° in specialist jumpers (those that use the jump as a usual form of locomotion) and 30° or lower in general jumpers (those that jump to escape from predators, and exceptionally to capture preys). Second, the body's centre of mass is accelerated until the take-off instant through an orientation that remains constant. The forelimbs do not participate in the propulsion that is only provided by the hind limbs. Jumping performance results from a trade-off between many morphological factors: *(i)* the ratio between the mass of the hind limb extensor and the total body mass, or, in terms of mechanical work, the ratio between the muscular work *vs* the work required to accelerate the body's centre of mass (Scholz *et al*., 2006); *(ii)* the hind limb length relative to snout-vent length (SVL) (Losos *et al*., 2000; Legreneur *et al*., 2012b); *(iii)* the architecture of extensor muscles and their insertion on the skeleton (Biewener and Roberts, 2000); (*iv*) the degree of freedom of the pelvis along the axis passing through the ilio-sacral and sacro-urostylar articulations (Kargo *et al*., 2002). In a specialist jumper, *e.g*. the South American hylid *Hypsiboas boans*, femur and tibiofibular lengths are similar and close to 50% of SVL (A. Herrel pers. comm.), for a maximal jumping performance of 209 cm. In contrast, in generalist jumpers, such as *Anolis carolinensis* Voigt, 1832, these lengths are also similar to each other, but they represent only 19% of SVL for a maximal performance of about 21 cm (Legreneur *et al*., 2012a; Gillis *et al*., 2009). In *Triadobatrachus*, femoral and tibial relative lengths are respectively 24% and 16% of SVL. These values indicate that if *Triadobatrachus* jumped, it would have been a general jumper as proposed by RR89. Jumping capacity is highly related with tibiofibula to femur ratio value. Zug (1972) reported that strong jumpers have a ratio above one, *i.e*. 1.14 and 1.13 for *Pseudacris crucifer* and *Rana clamitans* respectively, whereas weak jumpers have a ratio below one, *i.e*. 0.99 for *Bufo terrestris*. In *Triadobatrachus*, tibiofibula to femur ratio value is 0.66, which suggests that its jumping performance was poor. Moreover, the lack of fusion of the tibiofibula is not compatible with achieving great jumping performance (Roček and Rage, 2000).

In extant anurans, a functional relationship exists between sacroiliac configuration and locomotion (Reilly and Jorgensen, 2011). In *Triadobatrachus*, the ilia are moderately elongated and in the sacroiliac articulation, we cannot determine whether the sacral ribs were located dorsal to the anterior rami of the ilia ('narrow configuration') or between them ('broad configuration'). However, neither configuration would fit the categories recognised for anurans, *i.e*. fore-aft-slider, lateral bender, or sagittal hinge. Therefore, the locomotor function of the basin must be inferred from assumptions about morphology. According to RR89, hind limb muscle insertion areas were not affected by the prolongation of the anterior rami of the ilia. RR89 also suggested that the pubis could have played a shock absorber role in jumping. However, as discussed above, in quadrupedal tetrapods, generalist jumpers always land on their forelimbs. It therefore seems that, if the mobility of the basin was sufficient around the sacroiliac joint, its function would be to act as an additional member to create mechanical power during the impulsion (Kargo *et al*., 2002).

During impulsion, the horizontal distance between the vertical projection of the body's centre of mass of the animal and the centre of pressure (point located between the hindlimb and the floor at which the ground reaction force is applied) generates a rotational momentum at take-off. The longer the distance between these two points is, the greater the momentum is. Thus, this torque depends on the length of the hindlimbs, the SVL, the position of the body's centre of mass, and the orientation of the velocity vector at takeoff instant. In *Pelophylax* kl. *esculentus* (Nauwelaerts and Aerts, 2006), this distance is relatively short because of its body proportions (short SVL, long

hindlimbs) and a takeoff angle near 45°. However, the rotation torque is present and induces a rotation of the body of the frog of about 40° during a typical jump. This allows the animal to take off with the hindlimbs and land on the forelimbs. In the squamate *Anolis carolinensis*, whose hindlimb length and SVL are closer to those of *Triadobatrachus*, a similar rotation is observed in spite of longer SVL, shorter hindlimbs and lower take-off velocity orientation. Indeed, these parameters should induce a greater rotation torque. In fact, this torque is compensated by the presence of the tail that moves back the position of the animal's centre of gravity. Thus, in case of autotomy, forward rotation of *A. carolinensis* increases to about 110º, inducing a loss of control of the body during the aerial phase and landing on the back (Higham *et al*., 2001; Gillis *et al*., 2009). These studies suggest that the tail can be used actively in the aerial phase to correct the body position in three dimensions. As shown above, *Triadobatrachus* probably lacked a protruding tail, and even if it protruded, the tail would have been too short to have served that function. Thus, if we suppose that it was able to jump, its long SVL, relatively short hindlimbs and its generalist jumper behaviour with take-off angle below 30° would induce a momentum that could not be compensated during the aerial phase because of the lack of a tail. Therefore, jumping as escape behaviour in trophic interactions would have been disadvantageous for *Triadobatrachus*.

In conclusion, phenotypic traits of *Triadobatrachus* suggest that it would have had trouble to jump efficiently, although its forelimbs would have enabled it to land adequately. This interpretation is consistent with RR89's conclusions about the locomotion of *Triadobatrachus*, and their hypothesis that early salientian evolution was not driven by specialisation for efficient jumping. Instead, these morphological traits seem to indicate a walker/hopper behaviour in *Triadobatrachus* (Enriquez-Urzelai *et al*., 2015). This behaviour gives extant anurans a great capacity for sustained locomotion as active foragers (Wells, 2007). Maganuco *et al*. (2009) concluded that the palaeofloral assemblages of the Early Triassic of the Ambilobe basin (where *Triadobatrachus* was found) are consistent with riparian forests or woodlands in open floodplains, a suitable environment for a walker/hopper.

Evolution of trunk length

Our analyses of the number of presacral vertebrae support the hypothesis that early batrachians and/or their immediate ancestors underwent significant trunk length reduction before the divergence between caudates and salientians, and that the trunk length of *Triadobatrachus* reflects mostly the ancestral condition, rather than a reduction specific to Salientia. The mean estimates for the ancestral number of presacrals in the basalmost nodes in caudates and salientians are identical or just one vertebra shorter (rounding off the decimals) than the mean estimate of 16 for the ancestral condition of batrachians. This suggests that the presacral number at the base of both clades is largely inherited from their recent common ancestor, with perhaps only a small amount of convergence. Marjanović and Laurin (2008) had estimated a maximum of 17 presacrals as the primitive state of the Caudata, appealing to a criterion of parsimony. Our results are concordant with their estimate, although the upper bounds of our 95% confidence round off to 19. The resolution of the polytomies at the base of Caudata, notably the position of *Hylaeobatrachus croyii* Dollo, 1884, could provide narrower estimates.

The estimates of ancestral presacral length/skull width ratio are more tentative given the nature and incompleteness of our data, but they also provide partial support to the idea of *Triadobatrachus* featuring a mostly plesiomorphic relative trunk length. Ten out of twelve of our estimates indicate no more than a 20% reduction of the trunk length of *Triadobatrachus* relative to the ancestral batrachian value. Only the analyses using the divergence dates from Pyron (2011) and San Mauro (2010) suggested a more drastic ~40% reduction. However, Pyron's (2011) dates derive from the first application of 'total evidence' dating to any empirical dataset, and must consequently be viewed with caution. The evolutionary model used for the phenotypic data in Pyron's (2011) analysis may have overestimated the length of branches subtending various extinct taxa, which may have inflated the ages of several nodes. For instance, the oldest known stem-gymnophionan *Eocaecilia*, which displays few obvious autapomorphies, was inferred to be linked to the other (crown-) gymnophionans by a long branch spanning about 50 My, and the stem-urodele *Karaurus* is similarly linked to urodeles by a branch extending over about 35 My (Pyron 2011: fig. 4), all of which seems counter-intuitive.

While the confidence intervals of our ancestral value reconstructions fail to provide unambiguous support for our hypothesis of a short-trunk batrachian ancestor, the mean estimates show that the available evidence favours a short trunk under several schemes of

relationships and divergence times. We believe that these results cast a more than reasonable doubt over the previous scenario with an ancestor of salamander-like body proportions.

The origin and pace of the shortening of the vertebral column of salientians and other batrachians is of great relevance for the hypotheses about the origin of the anuran morphotype, with its highly specialised caudopelvic apparatus optimized for jumping. Previous works had assumed that the evolution of the elements of the system were more or less simultaneous. For instance, Handrigan and Wassersug (2007a) pointed to *Triadobatrachus* as evidence that trunk shortening was accompanied by the loss of the adult tail, and RR89 (see also Roček and Rage, 2000a; Roček and Rage, 2000b) assumed that the same shortening was related to the elongation of the ilia. The latter proposed that the anteroposterior elongation of the ilia of *Triadobatrachus* may have been caused by the shortening of the trunk (by a reduction in the number of presacrals) coupled with the need to maintain a certain distance between the pectoral and pelvic girdles. However, the early urodele *Beiyanerpeton* Gao and Shubin, 2012 (Late Jurassic) had similar presacral length/skull width ratios and the same number of presacrals as *Triadobatrachus*, and the Late Jurassic caudate *Karaurus* has even fewer presacrals (12 or 13) and a lower ratio. Yet, none of them display anteroposterior elongation of the ilia. It is unclear why the proposed biomechanical constraint would not affect these caudates as well.

If the trunk length of *Triadobatrachus* is close to the ancestral state of batrachians as a whole, as our results suggest, the case for the elongation of the ilia evolving as a biomechanical response to axial shortening becomes even weaker. Therefore, it is more likely that the initial elongation of the ilia of *Triadobatrachus* and salientians in general appeared first as a result of other selective pressures. The anuran condition was probably attained after a second phase of further trunk reduction and the specialisation to the jumping behaviour. Similarly, the typical, fairly slender body proportions of urodeles, which are often considered to have been inherited from their Paleozoic ancestors, appear instead to result from a reversal.

Triadobatrachus *as a calibration constraint for molecular divergence time analyses*

Triadobatrachus has been used several times for setting calibration constraints on divergence age analyses based on molecular clocks, either as a nodal (*e.g.* San Mauro *et al*., 2005; Marjanović and Laurin, 2007; Zhang and Wake, 2009; San Mauro, 2010) or tip constraint (Pyron, 2011). Given the recent publication of guidelines for justifying fossil calibrations (Parham *et al*., 2012), a few comments on the appropriateness of *Triadobatrachus* for that purpose are timely and likely useful for future studies. Furthermore, uncertainties in the exact provenance of the specimen (see section 'Geological context and age') makes a review of the recent stratigraphic literature of the relevant Permo-Triassic strata of Madagascar timely. Benton *et al*. (2015) recently did this, but here we give more details and update some information. Parham *et al*. (2012) proposed a five-step checklist for the justification of each constraint; we will briefly discuss each with respect to the minimal geological age of Lissamphibia, Batrachia, and Salientia, considering *Triadobatrachus* and *Czatkobatrachus*.

1. *Museum numbers of specimen(s) that demonstrate all the relevant characters and provenance data should be listed. Referrals of additional specimens to the focal taxon should be justified*. The voucher number of *Triadobatrachus* (MNHN.F.MAE 126) is univocal and readily available, its provenance data are however very incomplete by modern standards (see section *Geological context and age*). The holotype and other specimens of *Czatkobatrachus* have more complete provenance data both geographically and geologically (Evans and Borsuk-Białynicka, 1998).
2. *An apomorphy-based diagnosis of the specimen(s) or an explicit, up-to-date, phylogenetic analysis that includes the specimen(s) should be referenced. Triadobatrachus* has several characters that indicate a stem-anuran position, *e.g.* moderately anteroposteriorly elongated iliac shafts with a dorsal tuberosity, moderately elongated metapodial elements, presence of a frontoparietal, transversally-oriented palatine, deeply triradiate pterygoid, presence of lateral alae of the parasphenoid, possible presence of a mentomeckelian, absence of teeth on the dentary. Futhermore, this position has been recovered in several phylogenetic analyses with widely different sampling foci (*e.g.* Gao and Wang, 2001; Vallin and Laurin, 2004; Pyron, 2011; Sigurdsen and Green, 2011). The holotype of *Czatkobatrachus* is an incomplete ilium featuring a moderately elongated shaft and a prominent dorsal tuberosity of anuran affinites. However, that specimen can afford only a very limited number of characters of phylogenetic

interest. Additional *Czatkobatrachus* specimens can be referred to improve that situation (scapular girdle elements being the most useful), but it should be considered that all the specimens are dissociated fragments whose attribution should be carefully justified given the presence of temnospondyls in the same assemblage.

3. *Explicit statements on the reconciliation of morphological and molecular data sets should be given*. While to a large extent, this matter is specific to the molecular data set of each analysis, we are aware of a single molecular phylogenetic analysis that is compatible with the paraphyly of Lissamphibia (Fong *et al*., 2012), and none for the paraphyly of Anura. The vast majority of molecular analyses are not discordant with recent morphological phylogenetic analyses and they pose no conflict for the phylogenetic position of *Triadobatrachus* and *Czatkobatrachus*.
4. *The locality and stratigraphic level (to the best of current knowledge) from which the calibrating fossil(s) was/were collected should be specified*. For *Triadobatrachus*, we have discussed this in detail in the section *Geological context and age*. Given those stratigraphic uncertainties (Late Induan – early Olenekian), we differ from Benton *et al*., 2015 in that we conservatively suggest to set minimum age of Batrachia and Lissamphibia at the top of the early Olenekian instead of the top of the Induan (the subdivisions of the Olenekian have not been dated precisely, see below). The holotype and all the other specimens of *Czatkobrachus* belong to the tetrapod assemblage collected from a single fissure known as 'Czatkowice 1', of the Early Triassic karst deposits of the Czatkowice 1 quarry. Shishkin and Sulej (2009) and Borsuk-Białynicka *et al*. (2003) recently dated the deposits of this fissure to the late Olenekian based on tetrapod fauna correlations. Thus, the fossils of *Czaktobatrachus* are stratigraphically more recent than that of *Triadobatrachus*. However, the temporal distance between them is so small that the two taxa may have overlapping true (rather than observed) stratigraphic ranges, and should have no effect for most molecular dating studies considering the magnitude of the associated errors.
5. *Reference to a published radioisotopic age and/or numeric timescale and details of numeric age selection should be given*. The 2013 edition of the ICS International Chronostratigraphic Chart (Cohen *et al*., 2013) gives a numerical age of 251.2 Ma for the end of the Induan and 247.2 Ma for the end of the Olenekian. The numeric ages of the subdivisions of these stages have not been precisely established; researchers should consult the most recent literature if they wish to work with that level of stratigraphic resolution. The specimen-based approach for calibration constraints endorsed by Parham *et al*. (2012) highlights the weaknesses for that end of *Triadobatrachus* (scant provenance data) and *Czatkobatrachus* (morphological incompleteness), but there is little doubt that given the available evidence the end of the early Olenekian should be set as a minimum age for Lissamphibia and Batrachia.

Conclusions

We hope that the present work represents a significant improvement of our knowledge of *Triadobatrachus*, but we have also revealed new problems. In particular, the sequence of modifications in the evolution of the salientian trunk and caudopelvic apparatus seems to contradict previous hypotheses, but we still have a very incomplete picture, and the functional implications remain enigmatic. We expect that this new perspective of this key salientian will stimulate further research.

Acknowledgements

We wish to thank Florent Goussard for technical assistance during the segmentation process, Damien Germain for discussions, and Salvador Bailon for access to the Zooarchaeology collection of the MNHN. Anthony Herrel, Daniel Moen and Menelia Vasilopoulou-Kampitsi shared with us data about the morphology and jumping performance of *Hypsiboas boans*. Jean-Philippe Blouet and Renaud Boistel provided helpful suggestions to improve early versions of parts of this manuscript, and Zbyněk Roček gave us insightful comments on a late draft. Jean-Sébastien Steyer helped with a comment on our review of the geological setting. Pim Arntzen, Alessandro Garassino, and L. Analía Púgener kindly sent us literature. Jason Anderson and two anonymous reviewers provided comments that helped to improve the quality of this article. The Paleobiology Database http://www.fossilworks.org and LISANFOS KMS (Martín and Sanchiz 2015) greatly facilitated the access to data and references. This study originated as E. Ascarrunz' master dissertation at the MNHN; he was funded by the 'Bourse Master' scholarship programme of the Conseil Régional d'Île-de-France during that period. J.-C. R. and M.L. were funded by recurring grants from the CNRS, the French Ministry of Research and Sorbonne Universités to the CR2P.

References

Anderson JS, Reisz RR, Scott D, Fröbisch NB, Sumida SS. 2008. A stem batrachian from the Early Permian of Texas and the origin of frogs and salamanders. *Nature* 453: 515-518. doi: 10.1038/nature06865

Báez AM, Basso NG. 1996. The earliest known frogs of the Jurassic of South America: Review and cladistic appraisal of their relationships. *Münchner Geowissenschaftliche Abhandlungen A* 30: 131-158.

Báez AM, Nicoli L. 2004. A new look at an old frog: The Jurassic *Notobatrachus* Reig from Patagonia. *Ameghiniana* 41: 257-270.

Bapst DW. 2012. paleotree: an R package for paleontological and phylogenetic analyses of evolution. *Methods in Ecology and Evolution* 3: 803-807. doi: 10.1111/j.2041-210X.2012.00223.x

Bapst DW. 2013. A stochastic rate-calibrated method for time-scaling phylogenies of fossil taxa. *Methods in Ecology and Evolution* 4: 724-733. doi: 10.1111/2041-210X.12081

Bapst DW. 2014. Assessing the effect of time-scaling methods on phylogeny-based analyses in the fossil record. *Paleobiology* 40: 331-351. doi: 10.1666/13033

Beaulieu JM, Jhwueng D-C, Boettiger C, O'Meara BC. 2012. Modeling stabilizing selection: Expanding the Ornstein-Uhlenbeck model of adaptive evolution. *Evolution* 66: 2369-2383. doi: 10.1111/j.1558-5646.2012.01619.x

Benton MJ, Donoghue PC, Asher RJ, Friedman M, Near TJ, Vinther J. 2015. Constraints on the timescale of animal evolutionary history. *Palaeontologia Electronica* 18: 1-106.

Besairie H. 1932. Sur le Permo-Trias marin du Nord de Madagascar et l'âge du Karroo. *Comptes rendus sommaires des séances de la Société Géologique de France* 10: 30-34.

Besairie H. 1972. Géologie de Madagascar. 1. Les terrains sédimentaires. *Annales géologiques de Madagascar* 35.

Besairie H, Collignon M. 1960. Madagascar (supplément). In: Afrique. Vol. 4. Lexique stratigraphique international. Paris: Centre National de la Recherche Scientifique.

Biewener AA, Roberts TJ. 2000. Muscle and tendon contributions to force, work, and elastic energy savings: A comparative perspective. *Exercise and Sport Sciences Reviews* 28: 99.

Blender - a 3D modelling and rendering package. 2014. Blender Online Community. Blender Foundation. Version 2.72b. http: //www.blender.org

Bolt JR. 1969. Lissamphibian origins: Possible protolissamphibian from the Lower Permian of Oklahoma. *Science* 166: 888-891. doi: 10.1126/science.166.3907.888

Borsuk-Białynicka M, Evans SE. 2002. The scapulocoracoid of an Early Triassic stem-frog from Poland. *Acta Palaeontologica Polonica* 47: 79-96.

Borsuk-Białynicka M, Maryańska T, Shishkin MA. 2003. New data on the age of the bone breccia from the locality Czatkowice 1 (Cracow Upland, Poland). *Acta Palaeontologica Polonica* 48: 153-155.

Boulenger GA. 1908. A revision of the Oriental pelobatid batrachians (Genus *Megalophrys*). *Proceedings of the Zoological Society of London* 78: 407-430. doi: 10.1111/j.1096-3642.1908.tb01852.x

Carroll RL. 2007. The Palaeozoic ancestry of salamanders, frogs and caecilians. *Zoological Journal of the Linnean Society* 150: 1-140. doi: 10.1111/j.1096-3642.2007.00246.x

Cignoni P, Ranzuglia G. 2014. MeshLab. Visual Computing Lab - ISTI - CNRS. http: //meshlab.sourceforge.net/

Cohen KM, Finney SC, Gibbard PL, Fan J-X. 2013. The ICS international chronostratigraphic chart. *Episodes* 36: 199-204.

Cosgriff JW. 1984. The temnospondyl labyrinthodonts of the earliest Triassic. *Journal of Vertebrate Paleontology* 4: 30-46. doi: 10.1080/02724634.1984.10011984

Dong L, Roček Z, Wang Y, Jones MEH. 2013. Anurans from the Lower Cretaceous Jehol Group of Western Liaoning, China. *PLoS ONE* 8: e69723. doi: 10.1371/journal.pone.0069723

Duméril AMC, Bibron G. 1841. Erpétologie générale ou histoire naturelle complète des reptiles. Paris: Librairie Roret.

Emerson SB. 1983. Functional analysis of frog pectoral girdles. The epicoracoid cartilages. *Journal of Zoology* 201: 293-308.

Emerson SB. 1988. Testing for historical patterns of change: A case study with frog pectoral girdles. *Paleobiology* 14: 174-186.

Emerson SB, De Jongh H. 1980. Muscle activity at the ilio-sacral articulation of frogs. *Journal of Morphology* 166: 129-144.

Enriquez-Urzelai U, Montori A, Llorente GA, Kaliontzopoulou A. 2015. Locomotor Mode and the Evolution of the Hindlimb in Western Mediterranean Anurans. *Evolutionary Biology* 42: 199-209.

Estes R, Reig OA. 1973. The early fossil record of frogs: A review of the evidence. In: Vial JL, editor. Evolutionary biology of the anurans: Contemporary research on major problems. Columbia: University of Missouri Press. pp. 11-63.

Evans SE, Borsuk-Białynicka M. 1998. A stem-group frog from the Early Triassic of Poland. *Acta Palaeontologica Polonica* 43: 573-580.

Fong JJ, Brown JM, Fujita MK, Boussau B. 2012. A Phylogenomic Approach to Vertebrate Phylogeny Supports a Turtle-Archosaur Affinity and a Possible Paraphyletic Lissamphibia. *PLoS ONE* 7: e48990. doi: 10.1371/journal.pone.0048990

Gao K-Q, Chen S. 2004. A new frog (Amphibia: Anura) from the Lower Cretaceous of western Liaoning, China. *Cretaceous Research* 25: 761-769. doi: 10.1016/j.cretres.2004.06.011

Gao K-Q, Wang Y. 2001. Mesozoic anurans from Liaoning Province, China, and phylogenetic relationships of archaeobatrachian anuran clades. *Journal of Vertebrate Paleontology* 21: 460-476. doi: 10.1671/0272-4634(2001)021[0460:MAFLPC]2.0.CO;2

Gardner JD, Roček Z, Přikryl T, Eaton JG, Blob RW, Sankey JT. 2010. Comparative morphology of the ilium of anurans and urodeles (Lissamphibia) and a re-assessment of the anuran affinities of *Nezpercius dodsoni* Blob *et al*., 2001. *Journal of Vertebrate Paleontology* 30: 1684-1696. doi: 10.1080/02724634.2010.521605

Gillis GB, Bonvini LA, Irschick DJ. 2009. Losing stability: Tail loss and jumping in the arboreal lizard *Anolis carolinensis*. *Journal of Expermiental Biology* 212: 604.

Griffiths I. 1956. Status of *Protobatrachus massinoti*. *Nature* 177: 342-343. doi: 10.1038/177342b0

Griffiths I. 1963. The phylogeny of the Salientia. *Biological Reviews* 38: 241-292. doi: 10.1111/j.1469-185X.1963.tb00784.x

Handrigan GR, Wassersug RJ. 2007a. The anuran Bauplan: A review of the adaptive, developmental, and genetic underpinnings of frog and tadpole morphology. *Biological Reviews* 82: 1-25. doi: 10.1111/j.1469-185X.2006.00001.x

Handrigan GR, Wassersug RJ. 2007b. The metamorphic fate of supernumerary caudal vertebrae in South Asian litter frogs (Anura: Megophryidae). *Journal of Anatomy* 211: 271-279. doi: 10.1111/j.1469-7580.2007.00757.x

Havelková P, Roček Z. 2006. Transformation of the pectoral girdle in the evolutionary origin of frogs: insights from the primitive anuran *Discoglossus*. *Journal of Anatomy* 209: 1-11. doi: 10.1111/j.1469-7580.2006.00583.x

Hecht MK. 1962. A reevaluation of the early history of the frogs. Part I. *Systematic Zoology* 11: 39-44. doi: 10.2307/2411448

Heckert AB, Mitchell JS, Schneider VP, Olsen PE. 2012. Diverse new microvertebrate assemblage from the Upper Triassic Cumnock Formation, Sanford Subbasin, North Carolina, USA. *Journal of Paleontology* 86: 368-390. doi: 10.1666/11-098.1

Herrel A, Gonwouo L, Fokam E, Ngundu W, Bonneaud C. 2012. Intersexual differences in body shape and locomotor performance in the aquatic frog, *Xenopus tropicalis*. *Journal of Zoology* 287: 311-316.

Higham TE, Davenport MS, Jayne BC. 2001. Maneuvering in an arboreal habitat: The effects of turning angle on the locomotion of three sympatric ecomorphs of *Anolis* lizards. *Journal of Experimental Biology* 204: 4141-55.

Ivakhnenko MF. 1978. Caudates from the Triassic and Jurassic of Middle Asia. *Paleontologicheskii Zhurnal* 3: 84-89.

Jacobs R, Ingen Schenau GJ van. 1992. Control of an external force in leg extensions in humans. *Journal of Physiology* 457: 611-26.

Kargo WJ, Nelson F, Rome LC. 2002. Jumping in frogs: Assessing the design of the skeletal system by anatomically realistic modeling and forward dynamic simulation. *Journal of experimental Biology* 205: 1683-1702.

Kozur HW. 2006. Remarks to the base of the Olenekian. *Albertiana* 34: 66-72.

Laloy F, Rage J-C, Evans SE, Boistel R, Lenoir N, Laurin M. 2013. A re-interpretation of the Eocene anuran *Thaumastosaurus* based on microCT examination of a "mummified" specimen. *PLoS ONE* 8: e74874. doi: 10.1371/journal.pone.0074874

Lanza B, Arntzen JW, Gentile E. 2010. Vertebral numbers in the Caudata of the western Palaearctic (Amphibia). *Atti del Museo Civico di Storia Naturale Trieste* 54: 3-114.

Laurin M. 1998. The importance of global parsimony and historical bias in understanding tetrapod evolution. Part I. Systematics, middle ear evolution and jaw suspension. *Annales des Sciences Naturelles - Zoologie et Biologie Animale* 19: 1-42. doi: 10.1016/S0003-4339(98)80132-9

Legreneur P, Homberger DG, Bels V. 2012. Assessment of the mass, length, center of mass, and principal moment of inertia of body segments in adult males of the Brown Anole (*Anolis sagrei*) and Green, or Carolina, Anole (*Anolis carolinensis*). *Journal of Morphology* 273: 765-775.

Legreneur P, Laurin M, Monteil K, Bels V. 2012. Convergent exaptation of leap up for escape in distantly related arboreal amniotes. *Adaptive Behavior* 20: 69-79.

Legreneur P, Thévenet F, Monteil K, Montuelle SJ, Pouydebat E, Bels V. 2010. Hindlimb interarticular coordinations in *Microcebus murinus* in maximal leaping. *Journal of Experimental Biology* 213: 1320-1327.

Lehmann JP, Chateau C, Nauche M. 1959. Paléontologie de Madagascar XXVIII. Les poissons de la Sakamena moyenne. *Annales de Paléontologie* 45: 117-219.

Litvinchuk SN, Borkin LJ. 2003. Variation in number of trunk vertebrae and in count of costal grooves in salamanders of the family Hynobiidae. *Contributions to Zoology* 72: 195-210.

Losos JB, Creer D, Glossip R, Goellner A, Hampton G, Roberts N, Haskell P, Taylor P, Etling J. 2000. Evolutionary implications of phenotypic plasticity in the hindlimb of the lizard *Anolis sagrei*. *Evolution* 54: 301-305.

Lucas SG. 2010. The Triassic timescale based on nonmarine tetrapod biostratigraphy and biochronology. *Geological Society, London, Special Publications* 334: 447-500. doi: 10.1144/SP334.15

Maddin HC, Anderson JS. 2012. Evolution of the amphibian ear with implications for lissamphibian phylogeny: insight gained from the caecilian inner ear. *Fieldiana Life and Earth Sciences* 5: 59-76. doi: 10.3158/2158-5520-5.1.59

Maganuco S, Steyer J-S, Pasini G, Boulay M, Lorrain S, Bénéteau A, Auditore M. 2009. An exquisite specimen of *Edingerella madagascariensis* (Temnospondyli) from the Lower Triassic of NW Madagascar: Cranial anatomy, phylogeny, and restorations. *Memorie della Società Italiana di Scienze Naturali e del Museo Civico di Storia Naturale di Milano* 36: 3-72.

Maglia AM, Pugener LA, Mueller JM. 2007. Skeletal morphology and postmetamorphic ontogeny of *Acris crepitans* (Anura: Hylidae): A case of miniaturization in frogs. *Journal of Morphology* 268: 194-223. doi: 10.1002/jmor.10508

Marjanović D, Laurin M. 2007. Fossils, molecules, divergence times, and the origin of lissamphibians. *Systematic Biology* 56: 369-388. doi: 10.1080/10635150701397635

Marjanović D, Laurin M. 2008. A reevaluation of the evidence supporting an unorthodox hypothesis on the origin of extant amphibians. *Contributions to Zoology* 77: 149-199.

Marjanović D, Laurin M. 2013. The origin(s) of extant amphibians: a review with emphasis on the "lepospondyl hypothesis". *Geodiversitas* 35: 207-272.

Marjanović D, Laurin M. 2014. An updated paleontological timetree of lissamphibians, with comments on the anatomy of Jurassic crown-group salamanders (Urodela). *Historical Biology* 26: 535-550. doi: 10.1080/08912963.2013.797972

Martín C, Sanchiz B. 2014-2015. Lisanfos KMS version 1.2. Online reference accessible at http: //www.lisanfos.mncn.csic.es/. Museo Nacional de Ciencias Naturales, MNCN-CSIC. Madrid, Spain.

McGowan GJ. 1998. The development and function of the atlanto-axial joint in albanerpetontid amphibians. *Journal of Herpetology* 32: 116-122. doi: 10.2307/1565490

McNeil AR. 2003. Principles of animal locomotion. Princeton: Princeton University Press.

McNeil AR, Bennet-Clark HC. 1977. Storage of elastic strain energy in muscle and other tissues. *Nature* 265: 114-7.

Nauwelaerts S, Aerts P. 2006. Take-off and landing forces in jumping frogs. *Journal of Experimental Biology* 209: 66-77.

Nauwelaerts S, Stamhuis E, Aerts P. 2005. Swimming and jumping in a semi-aquatic frog. *Animal Biology* 55: 3-15.

O'Meara BC, Ané C, Sanderson MJ, Wainwright PC. 2006. Testing for different rates of continuous trait evolution using likelihood. *Evolution* 60: 922-933. doi: 10.1111/j.0014-3820.2006.tb01171.x

Parham JF, Donoghue PCJ, Bell CJ, Calway TD, Head JJ, Holroyd PA, Inoue JG, Irmis RB, Joyce WG, Ksepka DT, *et al.* 2012. Best practices for justifying fossil calibrations. *Systematic Biology* 61: 346-359. doi: 10.1093/sysbio/syr107

Piveteau J. 1936. Origine et évolution morphologique des amphibiens anoures. *Comptes rendus de l'Académie de Sciences* 103: 1084-1086.

Piveteau J. 1937. Paléontologie de Madagascar. Un amphibien du Trias inférieur : Essai sur l'origine et l'évolution des amphibiens anoures. *Annales de Paléontologie* 26: 135-177.

Pugener LA. 2002. The vertebral column and spinal nerves of anurans. PhD thesis, University of Kansas.

Pyron RA. 2011. Divergence time estimation using fossils as terminal taxa and the origins of Lissamphibia. *Systematic Biology* 60: 466-481. doi: 10.1093/sysbio/syr047

Rage J-C. 2006. *Triadobatrachus* (Salientia, Amphibia), hier et aujourd'hui. *Annales de paléontologie* 92: 165-174. doi: 10.1016/j.annpal. 2006.03.008

Rage J-C, Roček Z. 1989. Redescription of *Triadobatrachus massinoti* (Piveteau, 1936) an anuran amphibian from the early Triassic. *Palaeontographica Abteilung A* 206: 1-16.

Rage J-C, Roček Z. 2007. A new species of *Thaumastosaurus* (Amphibia: Anura) from the Eocene of Europe. *Journal of Vertebrate Paleontology* 27: 329-336. doi: 10.1671/0272-463427

Reece JS, Mehta RS. 2013. Evolutionary history of elongation and maximum body length in moray eels (Anguilliformes: Muraenidae). *Biological Journal of the Linnean Society* 109: 861-875.

Reilly SM, Jorgensen ME. 2011. The evolution of jumping in frogs: Morphological evidence for the basal anuran locomotor condition and the radiation of locomotor systems in crown group anurans. *Journal of Morphology* 272: 149-168. doi: 10.1002/jmor.10902

Revell LJ. 2012. Phytools: An R package for phylogenetic comparative biology (and other things). *Methods in Ecology and Evolution* 3: 217-223. doi: 10.1111/j.2041-210X.2011.00169.x

Roček Z. 1981. Cranial anatomy of frogs of the family Pelobatidae Stannius, 1856, with outlines of their phylogeny and systematics. *Acta Universitatis Carolinae Biologica* 1980: 1-164.

Roček Z. 2003. Larval development and evolutionary origin of the anuran skull. In: Heatwole H, Davies M, editors. Amphibian Biology. Vol 5. Osteology. Chipping Norton, New South Wales, Australia: Surrey Beatty & Sons. p. 1877-1995.

Roček Z, Rage J-C. 2000a. Proanuran stages (*Triadobatrachus*, *Czatkobatrachus*). In: Heatwole H, Carroll RL, editors. Amphibian Biology. Vol. 4. Palaeontology. Chipping Norton, New South Wales, Australia: Surrey Beatty & Sons. pp. 1283-1294.

Roček Z, Rage J-C. 2000b. Anatomical transformations in the transition from temnospondyl to proanuran stages. In: Heatwole H, Carroll RL, editors. Amphibian Biology. Vol. 4. Palaeontology. Chipping Norton, New South Wales, Australia: Surrey Beatty & Sons. pp. 1274-1282.

Ročková H, Roček Z. 2005. Development of the pelvis and posterior part of the vertebral column in the Anura. *Journal of Anatomy* 206: 17-35. doi: 10.1111/j.0021-8782.2005. 00366.x

Ruta M, Coates MI. 2007. Dates, nodes and character conflict: Addressing the lissamphibian origin problem. *Journal of Systematic Palaeontology* 5: 69-122. doi: 10.1017/S1477201 906002008

San Mauro D. 2010. A multilocus timescale for the origin of extant amphibians. *Molecular Phylogenetics and Evolution* 56: 554-561. doi: 10.1016/j.ympev.2010.04.019

San Mauro D, Vences M, Alcobendas M, Zardoya R, Meyer A. 2005. Initial diversification of living amphibians predated the breakup of Pangaea. *The American Naturalist* 165: 590-599. doi: 10.1086/429523

Schoch RR. 2013. The evolution of major temnospondyl clades: an inclusive phylogenetic analysis. *Journal of Systematic Palaeontology* 11: 673-705. doi: 10.1080/14772019. 2012. 699006

Scholz MN, Bobbert MF, Knoek van Soest AJ. 2006. Scaling and jumping: Gravity loses grip on small jumpers. *Journal of Theoretical Biology* 240: 554-61.

Shen Y, Garassino A, Teruzzi G. 2002. Studies on Permo-Trias of Madagascar. 4. Early Triassic conchostracans from Madagascar. *Atti della Società Italiana di Scienze Naturali e del Museo Civico di Storia Naturale in Milano* 143: 3-11.

Shishkin MA, Sulej T. 2009. The Early Triassic temnospondyls of the Czatkowice 1 tetrapod assemblage. *Palaeontologia Polonica* 65: 77.

Shubin NH, Jenkins FA. 1995. An Early Jurassic jumping frog. *Nature* 377: 49-52. doi: 10.1038/377049a0

Sigurdsen T. 2008. The otic region of *Doleserpeton* (Temnospondyli) and its implications for the evolutionary origin of frogs. *Zoological Journal of the Linnean Society* 154: 738-751. doi: 10.1111/j.1096-3642.2008.00459.x

Sigurdsen T, Green DM. 2011. The origin of modern amphibians: A re-evaluation. *Zoological Journal of the Linnean Society* 162: 457-469. doi: 10.1111/j.1096-3642.2010.00 683.x

Sigurdsen T, Green DM, Bishop PJ. 2012. Did *Triadobatrachus* jump? Morphology and evolution of the anuran forelimb in relation to locomotion in early salientians. *Fieldiana Life and Earth Sciences*: 77-89. doi: 10.3158/2158-5520-5.1.77

Stipaničić PN, Reig OA. 1955. Breve noticia sobre el hallazgo de anuros en el denominado 'Complejo porfírico de la Patagonia extraandina' con consideraciones acerca de la composición geológica del mismo. *Revista de la Asociación Geológica Argentina* 10: 215-233.

Vallin G, Laurin M. 2004. Cranial morphology and affinities of *Microbrachis*, and a reappraisal of the phylogeny and lifestyle of the first amphibians. *Journal of Vertebrate Paleontology* 24: 56-72. doi: 10.1671/5.1

Vullo R, Rage J-C, Néraudeau D. 2011. Anuran and squamate remains from the Cenomanian (Late Cretaceous) of Charentes, western France. *Journal of Vertebrate Paleontology* 31: 279-291. doi: 10.1080/02724634.2011.550355

Wang Y. 2004. Taxonomy and Stratigraphy of Late Mesozoic Anurans and Urodeles from China. *Acta Geologica Sinica - English Edition* 78: 1169-1178. doi: 10.1111/j.1755-6724. 2004.tb00774.x

Watson DMS. 1941. VII. The origin of frogs. *Earth and Environmental Science Transactions of the Royal Society of Edinburgh* 60: 195-231. doi: 10.1017/S0080456800017877

Wells KD. 2010. The ecology and behavior of amphibians. University of Chicago Press.

Wignall PB, Twitchett RJ. 2002. Extent, duration, and nature of the Permian-Triassic superanoxic event. In: Koeberl C; McLeod KG, editors. Catastrophic Events and Mass Extinctions: Impacts and Beyond. Special papers. Boulder, Colorado: Geological Society of America. pp. 395-414.

Zhang P, Wake DB. 2009. Higher-level salamander relationships and divergence dates inferred from complete mitochondrial genomes. *Molecular Phylogenetics and Evolution* 53: 492-508.
Zug GR. 1972. Anuran locomotion: Structure and function. I. Preliminary observations on relation between jumping and osteometrics of appendicular and postaxial skeleton. *Copeia* 4: 613-624.

Received: 23 June 2015
Revised and accepted: 16 November 2015
Published online: 14 June 2016
Editor: R. Vonk

Online Supplementary Information

S1. UV photographs of *Triadobatrachus massinoti*. Major divisions of the scale in cm. JPEG image.

S2. 3D model 1. Whole fossil of *Triadobatrachus massinoti*. PDF 3D format. This version has been simplified (reduced number of polygons) to facilitate visualisation in most computers.

S3. 3D model 2. Reconstruction of the pelvic girdle in the narrow configuration.

S4. 3D model 3. Reconstruction of the pelvic girdle in the broad configuration.

S5. 3D model 1 in STL format. This version has not been simplified.

S6. Number of presacral vertebrae and presacral length/skull width ratio data and sources. Measurements given in different arbitrary units; only ratios are comparable. Plain text file in CSV format.
Non-bibliographic sources:
a) Photographs of specimens held at the UCL's Grant Museum of Zoology, University College London (prefix 'UCLGMZ'). Photographs available on the collection catalogue's website.
b) Specimens from the Comparative Anatomy Collection of Zooarchaeology of the MNHN, indicated by voucher number with prefix 'MNHN-ZA-AC'.
c) 'digimorph', stills of X-ray tomography scans from the Digital Morphology library website [http://www.digimorph.org/]. Only one of these specimens had a voucher number, but more details about their provenance are available on the website.
d) Cast of *Karaurus sharovi* held at the MNHN.

S7. References for the sources of file 6. File in BibTex format.

S8. Estimated global and local rates of evolution of trunk length calculated under the best-fit model. Plain text file in CSV format.

S9. Trees with estimated ancestral values and transformed branch lengths. Zip archive with files in Newick format. Estimated values are stored as node labels.